SYNTHESIS & CHARACTERISATION OF PANI-ZnO COMPOSITE

A thesis Submitted for the partial fulfillment of requirement for

the award of the degree of

MASTER OF TECHNOLOGY (M.Tech)

IN

MATERIAL SCIENCE & ENGINEERING

Submitted By

RAJEEV SEHRAWAT (60702016)

UNDER THE SUPERVISION OF

Dr. Kulvir singh
Asst.Prof
Thapar University
Patiala

Dr.ML Singla
Scientist G
Material Research Division
CSIO, Sector-30 C
Chandigarh

School of Physics &Materials Science (SPMS)

Thapar University

Patiala - 147001

June-2009

CERTIFICATE

This is hereby certify that the thesis entitled ***"SYNTHESIS AND CHARACTERISATION OF POLYANILINE-ZnO COMPOSITE"*** *submitted by* ***Mr. Rajeev Sehrawat,*** *THAPAR UNIVERSITY PATIALA (PUNJAB) is a record of research work carried out by him for the degree of* ***Master of Technology*** *under my guidance. This thesis is an original work of the candidate and to the best of my knowledge had not been submitted, in part or full, for any other degree or diploma in this or any other University. No portion of this thesis is a reproduction from any other source, published or unpublished, without acknowledgment.*

[Dr. Kulvir Singh]
Supervisor
School of Physics and Material science
Thapar university
Patiala

[Dr. M. L. Singla]
Scientist "G"
Material Research Division
Central Scientific Instruments Organisation
Sector-30 C, Chandigarh

Countersigned by:

Dr. O.P. Pandey
(Prof. & Head)
School of Physics and Material Science
Thapar University (Patiala)

Dr. R.K. Sharma
Dean of Academic Affairs
Thapar University
Patiala

ACKNOWLEDGEMENT

While pursuing my M.Tech degree, many seen and unseen hands pushed me forward; learned souls put me on the right path and enlightened me with their knowledge and experience. I shall remain grateful to all of them.

On submission of my thesis, I would like to express my esteemed sense of gratitude of my guides Dr. Kulvir Singh (Assist. Prof. School of Physics and Materials Science) and Dr. M.L. Singla (Scientist G Material Research Division C.S.I.O. Chandigarh) for their inspiration, encouragement and support through the work for their appreciation, suggestion, constructive criticism and providing me good concepts during my scientific endeavor.

I am grateful to Dr. O.P. Pandey Professor and Head School of Physics and Materials Science for his encouragement and execution of thesis work.

I would like to express my deep sense of guide to Dr. Pawan Kapur, Director C.S.I.O. for permitting me to work in the organization and to supplement my knowledge for successful completion of my dissertation work

I am also grateful to Mr. Manish Kumar Technical Assistant, for providing guidance throughout the process of my work. I am extremely thankful to the whole staff of MRD for there ever valuable guidance.

I would like to express my deep gratefulness to my parents and family who, in my ways encouraged me and provided me moral support.

Finally I would like to thank my co-partner Ms. Nidhi Rana for their invaluable ideas to the project and the work they have done to make the project reach this level.

Rajeev Sehrawat

[RAJEEV SEHRAWAT]

DEDICATED TO MY PARENTS

CONTENTS

LIST OF FIGURES

LIST OF PHOTOGRAPHS

LIST OF ACRONYMS

PANI	Polyaniline
PPy	Polypyrrole
ZnO	Zinc Oxide
APS	Ammonium Per Sulphate
ITO	Indium Tin Oxide
XRD	X-ray Diffraction
FTIR	Fourier Transformed Infrared Spectroscopy
TEM	Transmission Electron Microscope
TGA	Thermogravimetric Analysis
DSC	Differential Scanning Calorimeter
rpm	Rotation Per Minute
PANI-ZnO	Composite of Polyaniline and ZnO

LIST OF SYMBOLS

nm	Nanometrer
μm	Micrometer
mm	Millimeter
A^0	Angstrom
d	Interplaner distance
K	Kelvin
Ω	Ohm
R	Resistance
ρ	Resistivity
S/cm	Siemens per centimeter
mg/mL	Milligram per milliliter
t_g	Glass transition temperature
t	Time
^0C	Degree Celsius
eV	Electron volt
kV	Kilo volt
λ	Wavelength
ε	Dielectric constant

ABSTRACT

Films of polyaniline and PANI–ZnO composites have been synthesized by solution cast and spin coating technique. The ZnO powder of particle size 4 to 10nm was synthesized by sol–gel technique and the polyaniline was synthesized by chemical oxidative polymerization of aniline. The composite films were characterized by thickness measurement, X-ray diffraction (XRD), Thermogravimetry analysis(TGA), transmission electron microscopy (TEM) and Fourier transform infra red (FTIR) and the results were compared with polyaniline films. The thickness of film was found to be 4.9 micrometer, Thermogravimetry shows the change of weight with respect to temperature Dielectric properties of PANI and PANI–ZnO composite films have been investigated between frequency ranges of 1 to 800 kHz. The 'a' lattice parameter of ZnO was found to increase and the 'c' lattice parameter was found to decrease after ZnO–PANI composite formed. The characteristic FTIR peaks of PANI were found to shift to higher wave number in ZnO–PANI composite. These observed effects have been attributed to interaction of ZnO particles with PANI molecular chains. Dielectric constant of PANI–ZnO composite film was found to be smaller than the PANI film. Also on increasing the doping of ZnO nano-particles in PANI dielectric constant go on decreasing. The decrease of dielectric constant in PANI–ZnO films as compared to PANI was attributed to the interfaces formed between ZnO particles and PANI.

CHAPTER-1

INTRODUCTION TO CONDUCTING POLYMERS AND ITS COMPOSITE

CHAPTER-1

INTRODUCTION TO CONDUCTING POLYMERS AND ITS COMPOSITE

1.1 INTRODUCTION

This chapter deals with detail discussion about conducting polymers and the composites of the conducting polymers. Polyaniline is discussed in detail for its structure, synthesis and composite materials derived from it. Various applications of conducting polymers, their composites materials have also been discussed.

1.2. INTRODUCTION TO CONDUCTING POLYMERS

Polymers have emerged as one of the most important materials in the twentieth century. The twenty-first century will undoubtedly see the use of polymers move from primarily passive materials such as coatings and containers to active materials with useful optical, electronic, energy storage and mechanical properties. Indeed, this development has already begun with the discovery and study of conducting polymers [1].

Electronically conducting polymers possess a variety of properties related to their electrochemical behavior and are therefore active materials whose properties can be altered as a function of their electrochemical potential. The importance and potential impact of this new class of material was recognized by the world scientific community when Hideki Shirakawa, Alan J. Heeger and Alan G. MacDiarmid were awarded the Nobel Prize in Chemistry in 2000 for their research in this field [2-3]. Although these materials are known as new materials in terms of their properties, the first work describing the synthesis of a conducting polymer was published in the nineteenth century. At that time 'aniline black' was obtained as the product of oxidation of aniline, however, its electronic properties were not established [4].

The conducting polymers may be divided into three categories:

1. Redox polymer.

2. Ion conducting polymer.
3. Inherently conducting polymers.

Ionically conducting polymers (polymer/salt electrolytes) are of great interest because they exhibit ionic conductivity in a flexible but solid membrane. Ionic conductivity is different than the electronic conductivity of metals and conjugated conducting polymers, since current is carried through the movements of ions. They have been critical to the development of devices such as all-solid-state lithium batteries.

In 'conjugated conducting polymers', the redox sites are delocalized over a conjugated π system; however, 'redox polymers' have localized redox sites. The redox polymers are well known to transport electrons by hopping or self-exchange between donor and acceptor sites. The redox conductivity is comparatively lower than that of conjugated conducting polymers, likely due to slow electron transport to from the redox centre [1].

An organic polymer that possesses the electrical and optical properties of a metal while retaining its mechanical properties and processability, is termed an 'intrinsically conducting polymer' (ICP). These properties are intrinsic to the 'doped' form of the polymer. The conductivity of ICPs lies above that of insulators and extends well into the region of common metals; therefore, they are often referred to as 'synthetic metals.' The common feature of most ICPs is the presence of alternating single and double bonds along the polymer chain, which enable the delocalization or mobility of charge along the polymer backbone. The conductivity is thus assigned to the delocalization of π-bonded electrons over the polymeric backbone, exhibiting unusual electronic properties, such as low energy optical transitions, low ionization potentials and high electron affinities [5].

Of the many interesting conducting polymers that have been developed over the past 30 years, those based on polyanilines, polypyrroles, polythiophenes, polyphenylenes and poly(*p*-phenylene vinylene)s have attracted the most attention. Figure 1.1 shows the structure of some conjugated polymers in their neutral insulating form. In order to make them electronically conductive, it is necessary to introduce mobile carriers into the conjugated system; this is achieved by oxidation or reduction reactions and the insertion of counterions (called 'doping').

During the doping process, an organic polymer, either an insulator or semiconductor having small conductivity, typically in the range of 10^{-10} to 10^{-5} S/cm, is converted to a polymer which is in a 'metallic' conducting regime (1 to 10^4S/cm).

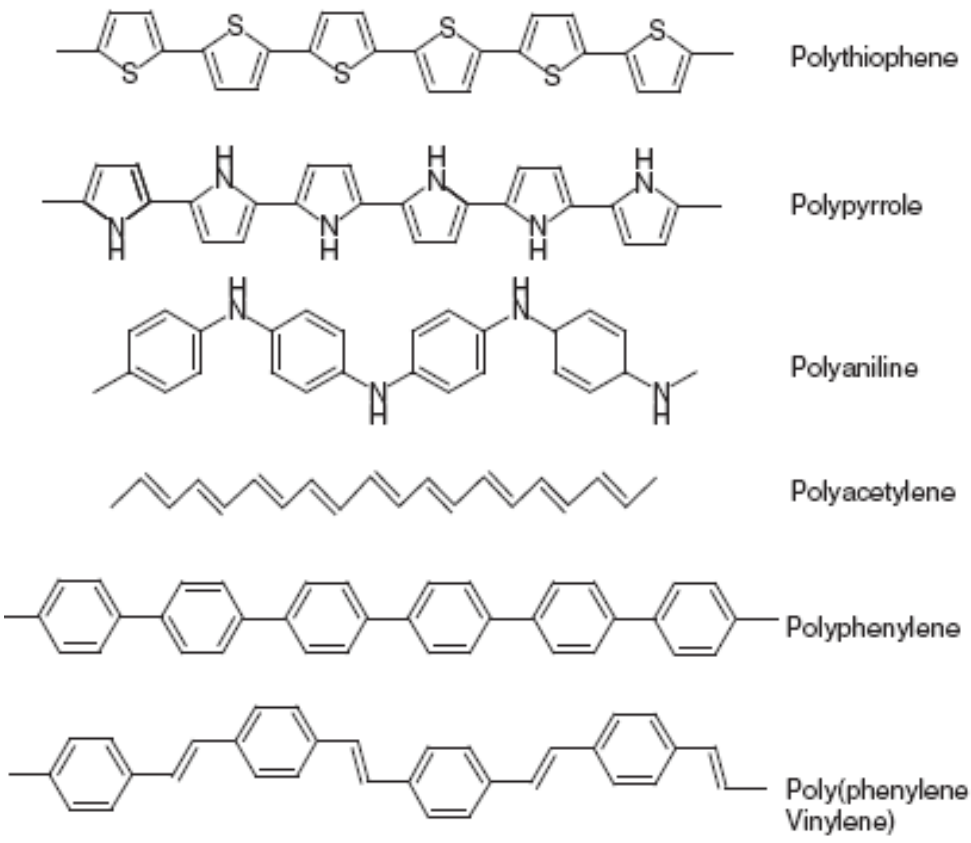

Fig 1.1 Structure of conjugated polymers

The highest value reported to date has been obtained in iodine-doped polyacetylene (>10^5 S/cm) and the predicted theoretical limit is about 2×10^7, more than an order of magnitude higher than that of copper [6]. Conductivity of other conjugated polymers reaches up to 10^3 S/cm [7, 8].

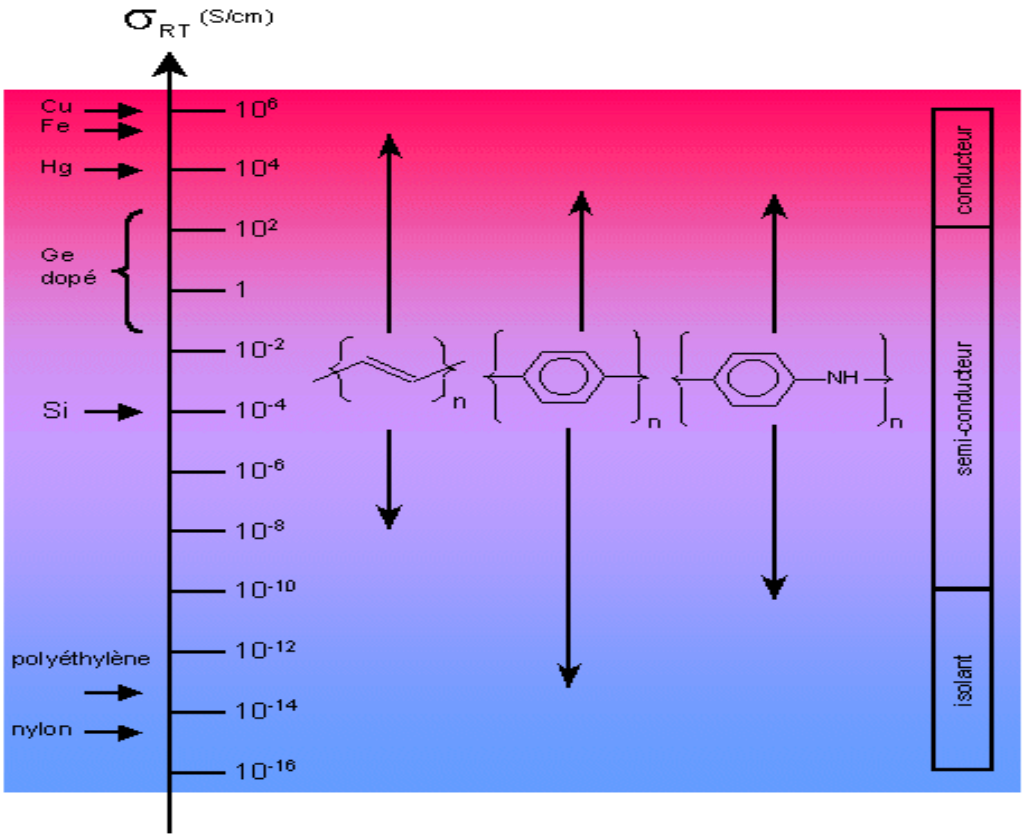

Fig.1.2 Conductivity of different materials

1.3 THEORY OF CONDUCTING POLYMERS

Conducting polymers are unusual in that they do not conduct electrons *via* the same mechanisms used to describe classical semiconductors and hence their electronic properties cannot be explained well by standard band theory. The electronic conductivity of conducting polymers results from mobile charge carriers introduced into the conjugated π-system through doping. To explain the electronic phenomena in these organic conducting polymers, new concepts including solitons, polarons and bipolarons have been proposed by solid-state physicists. The electronic structures of π-conjugated polymers with degenerate and nondegenerate ground states are different. In π-conjugated polymers with degenerate ground states, solutions are the important and dominant charge storage species [1]. Polyacetylene, (CH)x, is the only known polymer with a degenerate ground state due to its access to two possible configurations as shown in Figure 1.2.

The two structures differ from each other by the exchange of the carbon–carbon single and double bonds. While polyacetylene can exist in two isomeric forms: cis and trans-polyacetylene, the trans-acetylene form is thermodynamically more stable and the cis–trans isomerization is irreversible [9].

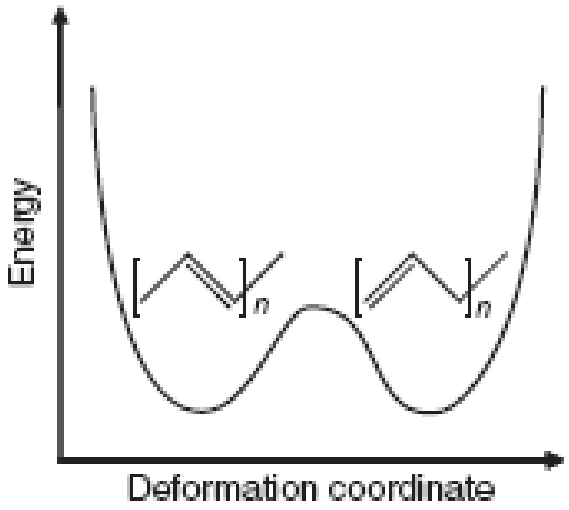

Fig.1.3 Energetically equivalent forms of degenerate polyacetylene.

Oxidative (p-type) doping of polyacetylene involves the chemical or anodic oxidation of the polymer to produce carbonium cations and radicals with simultaneous insertion of an appropriate number of anions between the polymer chains that neutralize the charge as shown in Figure 1.6 [10]. Two radicals can then recombine to give a spinless dication referred to as a positive soliton, which can act as the charge carrier [11]. Each soliton constitutes a boundary which separates domains that differ in the phase of their π-bonds. In solid-state physics a charge associated with a boundary or domain wall is called a soliton, because it has the properties of a solitary wave that can move without deformation and dissipation [12].

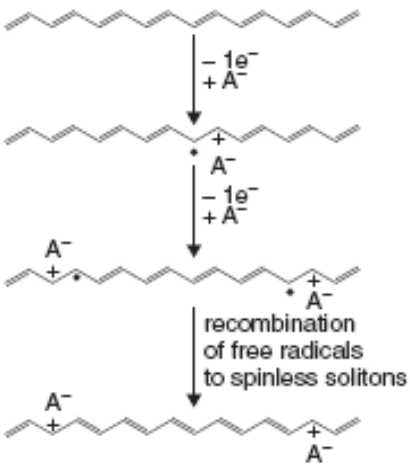

Fig.1.4 p-type doping in polyacetylene.

The π-conjugated systems based on aromatic rings, such as polythiophene, polypyrrole, polyaniline, polyparaphenylene and their derivatives have nondegenerate ground states. In these polymers, the ground-state degeneracy is weakly lifted so that polarons and bipolarons (confined soliton pairs) are the important and dominant charge storage configurations.

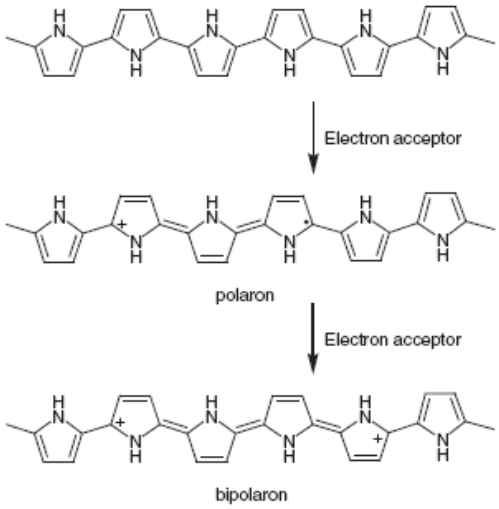

Fig.1.5 Polaron and bipolaron formation on π-conjugated Backbone of polypyrrole.

1.4 SYNTHESIS METHODS

Intrinsically conducting polymers are generally synthesized *via* chemical or electrochemical oxidation of a monomer where the polymerization reaction is stoichiometric in electrons. However, several other synthetic approaches exist, such as photochemical-initiated or biocatalytic oxidative polymerizations using naturally occurring enzymes.

1.4.1 Chemical Synthesis

Chemical synthesis has the advantage of being a simple process capable of producing bulk quantities of ICPs on a batch basis. To date it has been the major commercial method of producing such materials. Chemical polymerization is typically carried out with relatively strong chemical oxidants like ammonium peroxydisulfate, ferric ions, permanganate or bichromate anions, or hydrogen peroxide. These oxidants are able to oxidize the monomers in solution, leading to the formation of cation radicals. These cation radicals further react with other monomers or *n*-mers, yielding oligomers or insoluble polymer. There are two main limitations of the chemical oxidation technique, both related to the limited range of chemical oxidants available. The counterion of the oxidants ultimately ends up as a dopant or codopant in the polymer. Hence it is difficult to prepare ICPs with different dopants. The limited range of oxidants also makes it difficult to control the oxidizing power in the reaction mixture and in turn the degree of overoxidation during synthesis. Both the type of dopant and the level of doping are known to impact upon final properties of the polymer such as molecular weight, crosslinking and, ultimately, conductivity [1].

1.4.2. Electrochemical Synthesis

The electrochemical synthesis of conducting polymers, first demonstrated with polypyrrole [13], has proven important in the development of the field. Using this approach, semiconducting polymers have been obtained from a wide variety of monomers including thiophene, furan, carbazole, aniline, indole, azulene and polyaromatic monomers such as pyrene and fluoranthene. In general, chemical oxidation provides ICPs as powders, while electrochemical synthesis leads to films deposited on a working electrode. A wide range of anodes may be employed, including platinum, gold, carbon and indium-doped tin oxide (ITO)-coated glass.

1.5 POLYANILINE

Polyaniline has been the most intensively studied among the conducting polymers due to its unique properties, and this focus has resulted in significant development. Polyaniline shows reversible insulator-to-metal transitions and electrochromic behavior (yellow–green–blue–violet), depending on its oxidation state and pH. It has good stability in the presence of air and humidity. The combination of these characteristics makes polyaniline useful for various applications including rechargeable batteries [14], light emitting diodes [15], transistors [16], molecular sensors [17], nonlinear optical devices [18], corrosion protection [19], electromagnetic interference shielding [20], and electrochromic displays [21].

It exists in various oxidation states, Leucoemeraldine base, Emeraldine base Emeraldine salt and Pernigraniline

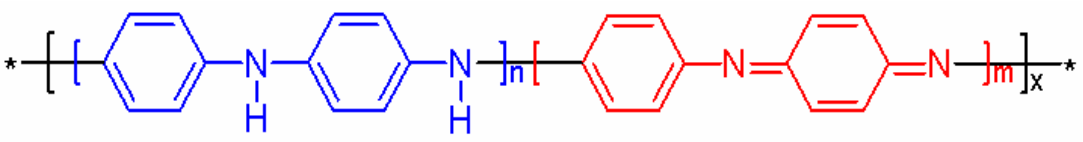

Fig.1.6 Structure of polyaniline

Polyaniline is a typical phenylene based polymer having a chemically flexible –NH group in a polymer chain flanked either side by a phenylene ring. It can also be defined as the simple 1, 4-coupling product of monomeric aniline molecule. The protonation and deprotonation and various other physico-chemical properties of polyaniline is due to the presence of the –NH- group. One of the most known and detailed investigated conducting polymer is polyaniline (PANI), a compound existing in many different oxidation states which conductivity strongly depends on protonation with organic or inorganic acids. The most common green protonated emeraldine has conductivity on a semiconductor level of the order of 100 S cm–1, many orders of magnitude higher than that of common polymers ($<10^{-9}$ S cm–1) but lower than that of typical metals ($>10^{4}$ S cm–1). Protonated PANI, (e.g., PANI hydrochloride) converts to a non-conducting blue emeraldine base when treated with ammonium hydroxide [22].

1.5.1 Synthesis of Polyaniline

The most common synthesis of polyaniline involves oxidative polymerization, in which the polymerization and doping occurs concurrently, and may be accomplished either electrochemically or chemically. Electrochemical methods tend to have lower yields than chemical yields.

Chemical Synthesis

Synthesis of polyaniline by chemical oxidative route involves the use of either hydrochloric or sulfuric acid in the presence of ammonium peroxo-di-sulfate as the oxidizing agent in the aqueous medium. The principal function of the oxidant is to withdraw a proton from an aniline molecule, without forming a strong co-ordination bond either with the substrate/intermediate or with the final product. However smaller quantity of oxidant is used to avoid oxidative degradation of the polymer formed. In the review article by Gospodinova et al. [23] they had reported that the propagation of polymer chains proceeds by a redox process between the growing chain (as an oxidant) and aniline (as a reducer) with addition of monomer to the chain end. The high concentration of a strong oxidant, $(NH_4)_2S_2O_8$, at the initial stage of the polymerization enables the fast oxidation of oligomer and polyaniline, as well as their existence in the oxidized form.

Electrochemical synthesis

The electrochemical preparation of conducting polymer dates back to early attempts of Dall'olio and coworkers [24], who obtained "pyrroleblack" as it was called at that time, on electrochemical oxidation of pyrrole in aqueous sulphuric acid as a powdery, insoluble ppt on a platinum electrode. Electrochemical polymerization is regarded as a simple and novel method for synthesis of conducting polymers.

The beauty of this method is that polymerization in suitable electrolytic medium gives directly the directly doped polymer as a flexible freestanding film. In this method, films are produced on the electrode surface by oxidative coupling. In this respect this method is somewhat similar to the electrochemical deposition of metal. the first electrochemical synthesis of polyemeraldine

salt was reported by Letheby in the year 1862. In the year 1962 Mohilner reported the mechanistic aspects of aniline oxidation. Major interest in the electrochemistry of polyaniline was generated only after the discovery that aromatic amine, pyrrole, thiophene, furan, indole and benzene can be polymerized anodically to conducting film. Elecrochemically prepared polyaniline is the preferred method to obtain a clean and better ordered polymer thin film.

1.6 COMPOSITES OF CONDUCTING POLYMERS

ICPs are 'doped conjugated polymers' and are fundamentally different from 'conducting polymer composites', 'redox polymers' and 'ionically conducting polymers' such as polymer/salt electrolytes. Conducting polymer composites are typically a physical mixture of a nonconductive polymer and a conducting material such as a metal or carbon powder distributed throughout the material. Conductive carbon blacks, short graphite fibers, and metal coated glass fibers, as well as metal particles or flakes, were used in early experiments for the preparation of such composites. Their conductivity is governed by percolation theory, which describes the movement of electrons between metallic phases and exhibits a sudden drop in conductivity (percolation threshold) at the point where the dispersed conductive phase no longer provides a continuous path for the transport of electrons through the material [1].

Now days a wide research has been carried out to synthesis the composites of polymer with nanostructures. The desire to synthesize nanostructures that combine the mechanical flexibility, optical and electrical properties of conducting polymers with the high electrical conductivity and magnetic properties of metal nanoparticles has inspired the development of several techniques for the controlled fabrication of metal nanoparticle—conducting polymer composites. Now, three main types of inorganic nanomaterials are used as inorganic fraction. The first interesting type is Metaloxide, which can improve the properties of PANI in the field of electricity, magnetism, etc.. The second type is metal nanoparticles. Up to now, many PANI/metal composites such as PANI/Au, PANI/Ag and PANI/Ni nanocomposites have been prepared using chemical or electrochemical method. The third main type of inorganic nanomaterials is carbon nanotube, which could improve the conductivity of PANI.

1.7 APPLICATIONS OF CONDUCTING POLYMERS

Conducting polymers are attractive materials for use in existing and emerging technologies due to their light weight, low cost and versatility compared with other standard conductors and semiconductors. Some examples of potential applications include rechargeable batteries, electrochromic displays and smart windows, light emitting diodes, toxic waste cleanup, sensors, field effect transistors and electromagnetic interference shielding, etc. Self-doped polymers are expected to play an important role in the technical implementation of conducting polymers since they can overcome many of the limitations associated with conducting polymers. For example, these polymers have proven to be an enabling step in the development of plastic electronic devices and biosensors.

The metal oxide semiconductor field effect transistor (MOSFET) is the most important device for very large scale integrated (VLSI) circuits such as microprocessors and memory devices. Much research has explored the use of conducting polymers as an active material in field effect transistor devices; dedoped or doped conjugated polymers such as trans-polyacetylene, polythiophene, thiophene oligomers, polythienylene vinylene, polyaniline [25] have all been demonstrated as suitable materials for field effect transistor architecture. The fig1.5 shows the cross sectional view of the MOSFET in which the active layer is made up of Polyaniline.

The second application field is in biosensor Polyaniline is conducting and electroactive only in its protonated (proton doped) form i.e., at low pH values. At pH values above 3 or 4, Polyaniline is insulating and electrochemically inactive. The use of self-doped Polyaniline and its derivatives could, in principle, enable the direct or mediated electron transfer between the polymer matrix and active centers of biocatalysts.

Next field of application is in electrochromic devices. In conducting polymers, the electrochromism, as well as the conductivity, is explained using band theory. The doping of a conducting polymer modifies its electronic structure, i.e., introduces charge carriers, producing new electronic states in the band gap, thus allowing new electronic transitions resulting in color changes.

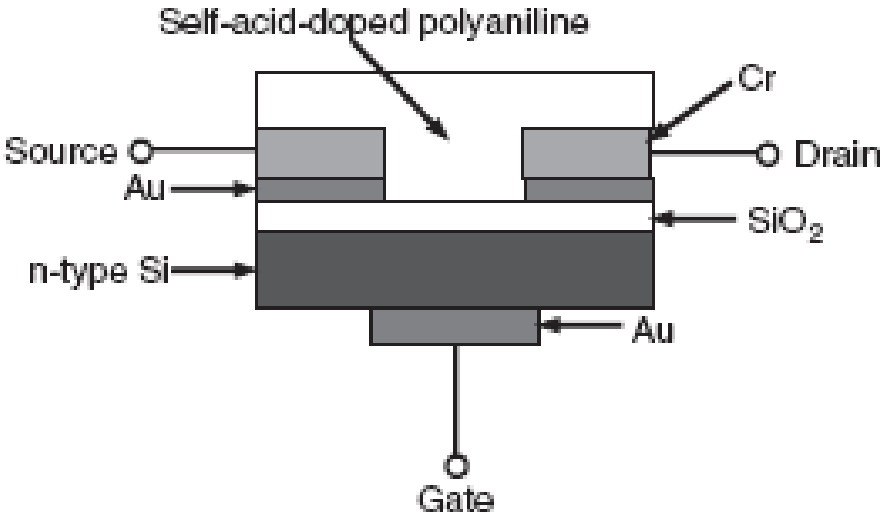

Fig.1.7 MOSFET with active of Polyaniline

A unique property of self-doped polymers is their ability to act as a 'charge controllable membrane' with cation exchange abilities in contrast to the anion exchange properties of classical polymers, i.e., doped with small or free moving anions. According to electrochemical analysis, the polymer has two separate oxidation states involving interactions of the polymer backbone with the covalently bound, self-doping, ion and counterions from the electrolyte, indicating that the polymer has the ability to act as a potential dependent, charge controllable, membrane with both cation exchange and anion exchange properties.

Lithium secondary batteries are one of the most important applications of electronically conducting polymers. Conducting polymers such as polyaniline, polypyrrole and polythiophene are expected to be promising materials for the electrodes of secondary batteries because they are relatively stable in air and have good electrochemical properties. In the discharging cycle of these batteries, the electrons flowing from the lithium anode (negative pole) through an external electric circuit must be consumed at the cathode (positive pole). When used as the active mass of a positive electrode, a conducting polymer ensures efficient utilization of electrons by converting

the oxidized form of the conducting polymer into the reduced form. Conversely, electrochemical oxidation of the reduced form takes place in the reverse charging cycle.

Controlled patterning of conducting polymers at a micro- or nanoscale is the first step towards the fabrication of miniaturized functional devices. Dip-pen nanolithography is a promising new nanofabrication tool, which allows one to pattern molecules on a variety of surfaces with a coated AFM tip in a controlled fashion on a sub-100nm to many micrometer scales. Researcher fabricated nanopatterns of self-doped conducting polyaniline by dippen nanolithography using electrostatic interactions as a driving force. The water soluble self-doped polyaniline 'ink' is converted to its solid state after patterning. The smallest feature size generated with these polymer inks had a diameter of 130 nm. In this case, the electrostatic interaction between the charged polymer chains and the oppositely charged substrate acts as a primary driving force in the dip-pen nanolithography process [1].

CHAPTER-2

LITERATURE REVIEW

CHAPTER-2
LITERATURE REVIEW

2.1 INTRODUCTION

This chapter includes the small description of the work of some research papers which are related to topic of my thesis. Some papers regarding polyaniline and its synthesis have been discussed. After it composite which are synthesized using polyaniline are discussed. At the end some work carried on the composites of PANI-ZnO has been discussed.

2.2 POLYANILINE

In 1990, Yue and Epstein [26] and Dao et al. [27] reported the first water soluble conducting derivatives of polyaniline, i.e., 'self-doped sulfonated polyaniline.' In this form, negatively charged sulfonate groups, covalently attached to the polymer backbone, act as intramolecular dopant anions which are able to compensate positive charges at protonated nitrogen atoms on the polymer backbone (Figure 2.1, A), thus replacing auxiliary solution dopant anions. This self-doped polymer is regarded as being created via the initial formation of the strong acid as shown in Figure 2.1, B. Benzenesulfonic acid is a strong acid, which protonates ('dopes') the imine nitrogen atoms to give conducting self-doped polymer in a manner analogous to the protonation of the parent emeraldine base form of polyaniline by HCl. This inner anion doping determines many of the distinctive properties of self- -doped polyaniline and distinguishes it from the parent polyaniline.

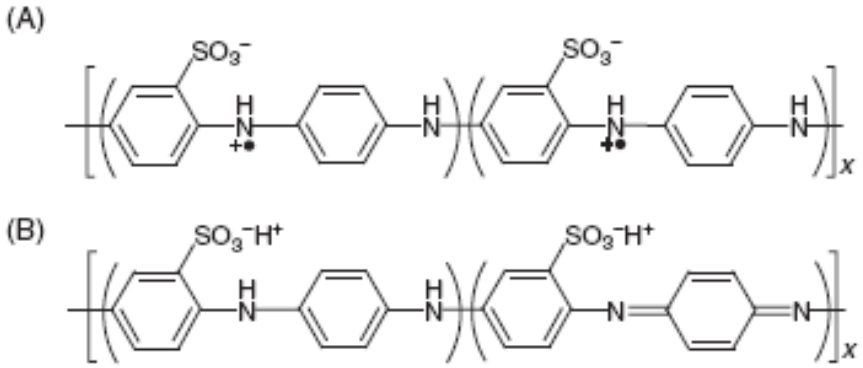

Fig.2.1 Structures of ring-sulfonated polyaniline.

Mathal et al. [28] prepared PANI films by ac plasma polymerization technique and studied its various properties and parameters like capacitance, dielectric loss, dielectric constant and the ac conductivity in the frequency range of 100 Hz to 1 MHz. They investigated that capacitance and dielectric loss decreased with frequency and increased with temperature.

Jakub et al. [29] discussed the changes in the electrical conductivity of polyaniline suspensions in 1,2,4-trichlorobenzene observed during the freezing and melting of the medium .They explained that by the changes in the organization of conducting particles in an electric field under a varying state of the system. The conductivity of liquid suspension was two orders of magnitude higher by comparison with the frozen one. Polyaniline suspensions were the new class of liquid systems comprising electrically conducting polymers. According to them, their electrical conductivity could be decreased by several orders of magnitude by freezing the suspension, while it was recovered after melting.

2.3. SYNTHESIS

Eight persons et al. [28] from five institutions in different countries carried out polymerizations of aniline. They oxidized aniline hydrochloride with ammonium peroxydisulphate in aqueous medium at ambient temperature. The yield of polyaniline was higher than 90 % in all cases. The electrical conductivity of polyaniline hydrochloride thus prepared was 4.4 to 1.7 S cm^{-1} (average of 59 samples), measured at room temperature. According to them, a product with defined

electrical properties could be obtained in various laboratories by following the same synthetic procedure.

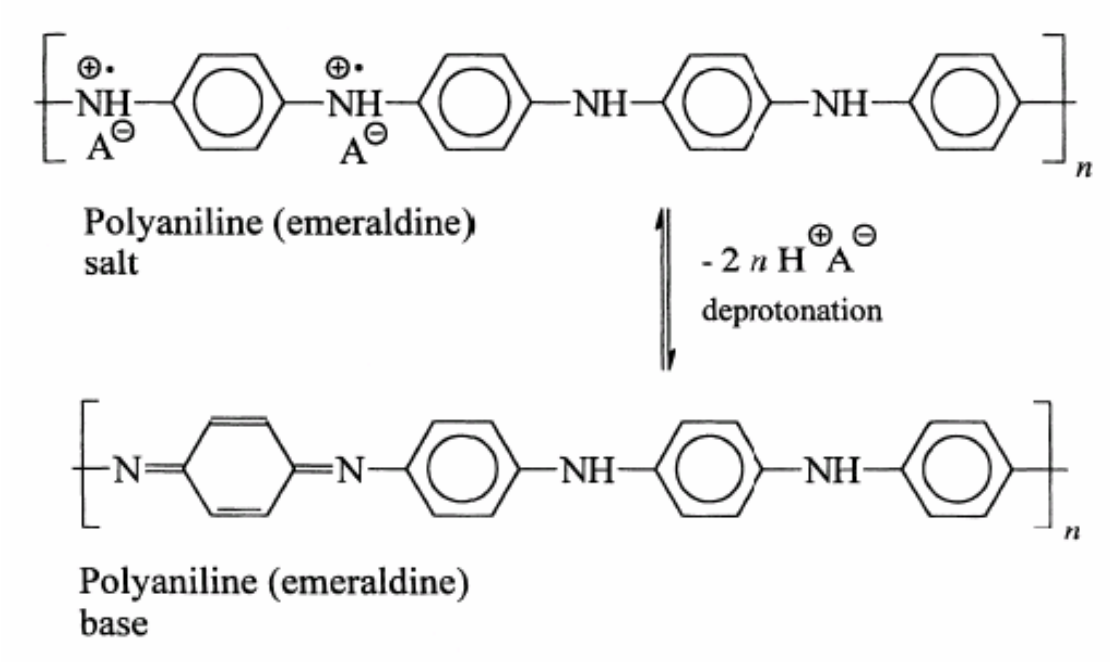

Fig.2.2 Polyaniline (emeraldine) salt is deprotonated in the alkaline medium to polyaniline (emeraldine) base.

Sacak et al. [30] Carried out that the conductive form of polyaniline was synthesized by the anodic and chemical oxidation of aniline in malonic acid medium. The conductivity of polyaniline doped with malonic acid changed from 1.62 x 10^{-6} to 2.5 x10^{-5} S cm^{-1} depending on the way it was synthesized. The polymer growth rate was observed to be very slow in malonic acid compared with H_2SO_4. Thermo gravimetric data revealed that the maximum thermal reaction rate of PANI doped with malonic acid was at 2000^oC and 5200^oC compared with 2900^oC and 5300^oC of the polymer doped with H_2SO_4. A conductive PANI can be synthesized in malonic acid solution using both chemical and electrochemical routes. The electrochemical polymer growth rate in malonic acid media was much slower than that observed in H_2SO_4.

2.4 COMPOSITE OF PANI

Hadi Nur [31] et al. prepared PANI/MCM-41-SO3H composites were successfully synthesized by in situ polymerization technique in the presence of aniline. HCl monomers as starting material. It is revealed that the long order integrity of MCM-41 remains intact after encapsulation of PANI. FTIR spectra of PANI in PANI/MCM-41-SO3H composites show that they are in the emeraldine salt form. Although PANI/MCM-41-SO3H composites show lower conductivity compared to PANI.DS, they show a higher thermal stability of conductivity than that of PANI.DS, because there is the interaction of the free electron pairs of the nitrogen atoms of the PANI with a charged molecule on the surface of MCM-41-SO3H with PANI. As a global guide for future actions, this work opens new perspectives for the use of PANI/MCM-41 composite as a conducting material at high temperature.

R. Del Riâo et al. [32] synthesized the composite of PANI and carbon black using electrochemical technique. The potential of Pt- electrode was varied and the electrode was dipped in the solution containing aniline and carbon black suspension. The solution may also contain sodium dodecyl sulphate (SDS) as additive. It is shown that the rate of polymerization is enhanced by the presence of both carbon black and SDS by a factor of 5. The composite was characterized by cyclic voltammetry, scanning electron microscopy and capacity measurements. PANI-CB composites were synthesized in 1 M HCl containing varying amounts of carbon black in suspension. SDS was used as additive in order to improve the stability and electroactivity of the films. The potential of the Pt working electrode was cycled between -0.2 and 0.8 V for 100 cycles at 0.1 Vs^{-1}, while stirring the electrolyte. Composites synthesized with SDS in the electrolyte were analyzed by electrochemical impedance spectroscopy (EIS) measurements in fresh 0.5 M H2SO4 solutions without the monomer. Carbon black and SDS in the forming electrolyte have a pronounced effect on the kinetics of polymerization. It is possible to obtain rather porous films in much shorter time than that employed to obtain films of PANI without any additive or carbon black. The presence of carbon black particles embedded in the polymer film does not seem to modify the intrinsic electronic properties of the composite, though the substantial increase in the composite film capacity is probably due to its higher surface area.

Y.-N. Qiat al. [33] synthesized Polyaniline/Al_2O_3 (PANI/Al_2O_3) composites by in-situ polymerization at the presence of HCl as dopant by adding Al2O3 nanoparticles into aniline solution. The composites were characterized by FTIR and XRD. The thermogravimetry (TG) and modulated differential scanning calorimetry (MDSC) were used to study the thermal stability and glass transition temperature (*T*g) of the composites, respectively. The results of FTIR showed that Al_2O_3 nanoparticles connected with the PANI chains and affected the absorption characteristics of the composite through the interaction between PANI and nano-sized Al_2O_3. And the results of XRD indicated that the peaks intensity of the PANI/ Al_2O_3 composite were weaker than that of the pure PANI. From TG and derivative thermogravimetry (DTG) curves, it was found that the pure PANI and the PANI/ Al_2O_3 composites were all one step degradation. And the PANI/ Al_2O_3 composites were more thermal stable than the pure PANI. The MDSC curves showed that the nano-sized Al_2O_3 heightened the glass transition temperature (*T*g) of PANI.

Neelgund et al. [34] prepared composites of polyaniline derivatives—polyaniline, poly(2,5-dimethoxyaniline) and poly(aniline-2,5-dimethoxyaniline)—and silver nanoparticles were through simultaneous polymerization of aniline derivative and reduction of $AgNO_3$ in the presence of poly(styrene sulfonic acid) (PSS). We used $AgNO_3$ as one of the initial components (1) to form the silver nanoparticles and (2) as an oxidizing agent for initiation of the polymerization reaction. UV-visible spectra of the synthesized nanocomposites reveal the synchronized formation of silver nanoparticles and polymer matrix. The morphology of the silver nanoparticles and degree of their dispersion in the nanocomposites were characterized by transmission electron microscopy. Thermogravimetric analysis and differential scanning calorimetry results indicate an enhancement of the thermal stability of the nanocomposites compared to the pure polymers. The electrical conductivity of the nanocomposites is in the range 10^{-4} to 10^{-2} S cm^{-1}.

2.5 COMPOSITE OF PANI-ZnO NANPARTICLES

Shiv P. Sharma et al. [34] advised a new method to synthesis the PANI-ZnO composite. This composite was used for a very different application. They used this composite for the oxidation of sulphides in the presence of H_2O_2 under solvent-free conditions. The results reveal that PANI-

ZnO composite has high activity and selectivity compared to the raw ZnO. The PANI-ZnO + H_2O_2 system may be envisaged as an efficient reagent in green sulphoxidation. The ZnO was synthesized chemically by using ammonium persulphate as oxidizing agent for the polymerization of the aniline monomer.

Ten milliliter aniline was dissolved in 150 ml distilled water containing 10 ml hydrochloric acid. The solution was cooled to 4–8 _C and the ZnO 19–21 g (1:2) was added to the solution and stirred thoroughly. (NH4)2S2O8 solution (5.4 g dissolved in 30 ml) was added to the reaction mixture so that the total volume was 200 ml. This was stirred for 30 min and allowed to stand for a further period of 60 min. The resultant product was filtered, washed thoroughly with water and dried until it showed constant weight at 50^{o}C. The composite ZnO-PANI (0.2 g) is mixed with liquid sulfide (1 mol). The resulting mixture is further treated with H_2O_2 (l equivalent, 30%). Then, the mixture is stirred for 20 min at room temperature.

Jui Hung Chen et al. [35] synthesized the composite of polystyrene and ZnO nanoparticles by Pickering emulsion method. ZnO nanoparticles were first prepared by reaction of zinc acetate and sodium hydroxide in ethanol medium. Then different amount of styrene monomer was emulsified in water in the presence of ZnO nanoparticles either by mechanical stirring or by sonication, followed by polymerization of styrene. Two kinds of initiators were used to start the polymerization, azobisisobutyronitrile (AIBN) and potassium persulfate (KPS). The X-ray diffraction pattern verified the crystal structure of ZnO and FTIR spectra evidenced the existence of ZnO and polystyrene (PS) in ZnO/polystyrene composite particles. Different morphologies were observed for the composite particles when using different initiators. From TEM photographs, AIBN-initiated system produced mainly core-shell composite particles with PS as core and ZnO as shell, while KPS-initiated system showed both composite particles and pure PS particles. Two schemes of reaction mechanism were proposed to explain the morphologies accordingly. Both systems of composite particles showed good pH adjusting ability.

Bhupendra K. Sharma et al. [37] developed the thin film of PANI and PANI-ZnO composite by solution casting and spin coating. The ZnO powder of particle size 100–200 nm was synthesized by sol–gel technique and the polyaniline was synthesized by chemical oxidative polymerization of aniline. The composite films were characterized by X-ray diffraction (XRD), scanning electron microscopy (SEM) and Fourier transform infra red (FTIR) and the results were compared with polyaniline films. Dielectric properties of PANI and PANI–ZnO composite films

have been investigated between frequency ranges of 8.5 and 13.0 GHz. The ‘a’ lattice parameter of ZnO was found to increase and the ‘c’ lattice parameter was found to decrease after ZnO–PANI composite formed. The characteristic FTIR peaks of PANI were found to shift to higher wave number in ZnO–PANI composite. These observed effects have been attributed to interaction of ZnO particles with PANI molecular chains. Dielectric constant of PANI–ZnO composite film was found to be smaller than the PANI film. The decrease of dielectric constant in PANI–ZnO films as compared to PANI was attributed to the interfaces formed between ZnO particles and PANI

CHAPTER-3

CHERACTERISATION TECHNIQUE AND EQUIPMENT USED

CHAPTER-3

CHERACTERISATION TECHNIQUE AND EQUIPMENT USED

3.1 INTRODUCTION

This chapter deals with the source and quality of chemical used during experimentation. Wherever necessary the methods of purification of chemicals are also described. The synthesis of ZnO nanoparticles, polyaniline PANI-ZnO composite and various techniques used to characterize the material are also discussed.

3.2 MATERIAL AND APPARATUS USED

3.2.1 Material used for the synthesis of PANI-ZnO composite

All the chemicals were used of AR grade. The chemicals list is given in table 3.1

Table 3.1: Chemicals used during the experimentation.

S.No.	Chemical Used	Symbol	Source
1	Aniline	C_6H_7N	Spectrochem PVT LTD. mumbai
2	Ammonium persulphate	$(NH_4)_2S_2O_8$	Sd-fine chemical mumbai
3	Hydrochloric acid	HCl	Spectrochem PVT LTD. Mumbai
4	Ammonia	NH_3	Spectrochem PVT LTD. mumbai
5	N-Methyl-2-Pyralodine	C_5H_9NO	Spectrochem PVT LTD. mumbai
6	Methanol	CH_3OH	Sd-fine chemical mumbai
7	Zinc Acetate	$C_4H_{10}O_6Zn$	Sd-fine chemical mumbai
8	Deionized water	H_2O	Elga pure lab equipment (resistivity~ 18 $M\Omega cm^{-1}$)
9	Potassium hydroxide	KOH	Merck Suprapur
10	Chloroform.	$CHCl_3$	Merck Suprapur

3.3 EQUIPEMENTS/INSTRUMENTS USED

The following instrument/equipment has been used for the synthesis of PANI- ZnO composite.

3.3.1 Electronic Weighing Machine

Accurate quantity of chemical can be measured by using **METTLER TOLEDO AX205** electronic weighing machine shown in fig 3.2. the maximum and minimum limit of machine was 205gm and 0.01mg, respectively.

This equipment was used to measure the accurate quantity of PANI powder, ZnO nanoparticles and Zinc Acetate.

3.3.2 Centrifuge Machine

The machine is used to separate the undissolved particles of PANI from solvent. This was carried out using SIGMA Laboratory centrifuge 3K3O at the speed of 8000 rpm for 10 minutes. This machine have the ability to reach the speed of 26000 rpm at nearly 0 ^{0}C.

This equipment is based upon the principle of centrifugal force. This force acts on the particles when they are under rotation. The direction of force is towards away from the center. The solution is placed in the centrifuge tubes and machine applies centrifugal force. Due to this force undissolved particles of PANI sticks with the walls of the tubes and settle down [38].

3.3.3 Magnetic stirrer

The magnetic stirrer is used several times in the experiment, like when mixing dry powder of PANI in NMP and during the doping of ZnO in PANI.

The equipment is based on the principle of electromagnetism. Here the electric current is used to produce magnetic field. This magnetic field was then used to rotate the magnetic bead which was placed inside the inside the solution. It can produce heating effect also.

3.3.4 Electrical Oven

This oven was used to dry the precipitate of PANI which was obtained after filtration and to dry the films obtained by solution casting (at 50^{o}C). This oven can achieve the temperature of 300^{o}C.

3.3.5 Filtration system

This equipment is used to filter the solution which has green precipitate of conducting PANI. During synthesis the PANI get precipitated when oxidizing agent is added to it. To separate these precipitate from solution this filter assembly is used. This assembly contains

1. Flask
2. Buckle funnel
3. Vacuum pump
4. Filter paper

Photograph 3.1 Filter assembly.

3.4 CHARACTERISATION TECHNIQUES

Various techniques have been used to characterize the thin film of PANI, PANI-ZnO composites and nanoparticles. These techniques are discussed one by one as follows:

3.4.1 X-ray diffraction

For X-ray diffraction we use PANalytical's X'Pert PRO X-ray diffractometer system. It is virtually unlimited in its capacity to adapt to changing circumstances that call for new measurement techniques, and new functionality.

A crystal diffracts an X-ray beam passing through it to produce beams at specific angles depending on the X-ray wavelength, the crystal orientation and the structure of the crystal. In the macroscopic version of X-ray diffraction, a certain wavelength of radiation will constructively interfere when partially reflected between surfaces (i.e., the atomic planes) that produce a path difference equal to an integral number of wavelengths. This condition is described by the Bragg law

This relation demonstrates that interference effects are observable only when radiation interacts with physical dimensions that are approximately the same size as the wavelength of the radiation. Since the distances between atoms or ions are on the order of 10^{-10}m (1Å), diffraction methods require radiation in the X-ray region of the electromagnetic spectrum, or beams of electrons or neutrons with similar wavelength [39-41]. So, through X-ray spectra one can identify and analyze any crystalline matter. The degree of crystallinity or order will conditionate the quality of the obtained result.

In order to do this, a diffractometer is needed. Basically, an X-ray diffractometer consists in an X-ray generator, a goniometer and sample holder and an X-ray detector, such as photographic film or a movable proportional counter. The most usually employed instrument to generate X-rays is X-ray tubes, which generate X-rays by bombarding a metal target with high energy (10-100keV) electrons that knock out core electrons. Thus, an electron in an outer shell fills the hole in the inner shell and emits an X-ray photon. Two common targets are Mo and Cu, which have

strong K shell X-ray emissions at 0.71073 and 1.5418Å, respectively. Apart from the main line, other accompanying lines appear, which have to be eliminated in order to facilitate the interpretation of the spectra. These are partially suppressed by using crystal monochromators. In this case the powder provides all the possible orientations of the small crystals giving rise to a large number of diffraction cones, each one corresponding to a family of planes satisfying the Bragg's law. For large grains, rings are discontinuous and formed by small spots. As the size of the grains diminishes, the spots are closer and for an optimum size a continuous ring is obtained, which is transferred into a peak when working with graphic registers or lines in a photographic register. For lower grain sizes the clarity of rings is lost again and wide peaks or bands appear. When the crystals are not randomly but preferentially oriented the intensity of the different rings and along each ring is not uniform.

3.4.2 Fourier Transform Infrared Spectroscopy (FTIR)

FTIR spectra was recorded using Perkin Elmer RX-1 FTIR spectrophotometer in the range 500 cm^{-1} to 3500 cm^{-1}. The sample powder was first mixed with KBr, and then with the help of compressor it was converted in the form of pallet.

FTIR is most useful for identifying chemicals that are either organic or inorganic. It can be utilized to quantitate some components of an unknown mixture. It can be applied to the analysis of solids, liquids, and gasses. The term Fourier Transform Infrared Spectroscopy (FTIR) refers to a fairly recent development in the manner in which the data is collected and converted from an interference pattern to a spectrum. Today's FTIR instruments are computerized which makes them faster and more sensitive than the older dispersive instruments.

FTIR can be used to identify chemicals from spills, paints, polymers, coatings, drugs, and contaminants. FTIR is perhaps the most powerful tool for identifying types of chemical bonds (functional groups). The wavelength of light absorbed is characteristic of the chemical bond as can be seen in this annotated spectrum.

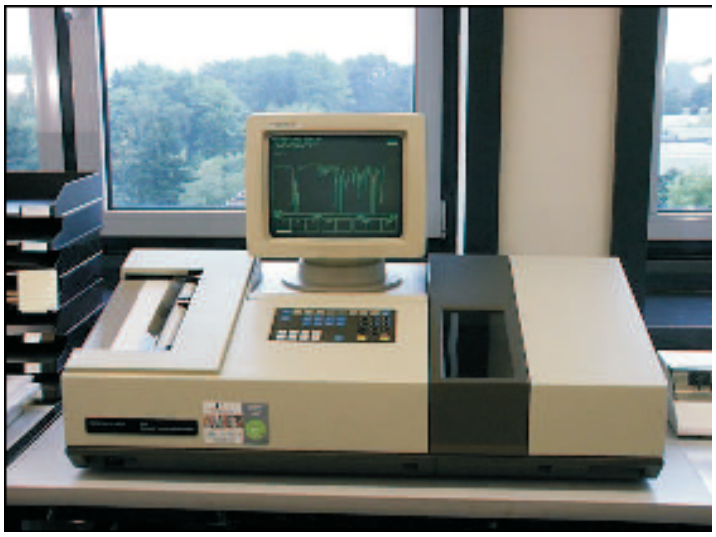

Photograph 3.2 FTIR spectrophotometer .

By interpreting the infrared absorption spectrum, the chemical bonds in a molecule can be determined. FTIR spectra of pure compounds are generally so unique that they are like a molecular "fingerprint". While organic compounds have very rich, detailed spectra, inorganic compounds are usually much simpler. For most common materials, the spectrum of an unknown can be identified by comparison to a library of known compounds. WCAS has several infrared spectral libraries including on-line computer libraries. To identify less common materials, IR will need to be combined with nuclear magnetic resonance, mass spectrometry, emission spectroscopy, X-ray diffraction, and/or other techniques

Because the strength of the absorption is proportional to the concentration, FTIR can be used for some quantitative analyses. Usually these are rather simple types of tests in the concentration range of a few ppm up to the percent level. For example, EPA test methods 418.1 and 413.2 measure the C-H absorption for either petroleum or total hydrocarbons. The amount of silica trapped on an industrial hygiene filter is determined by FTIR using NIOSH method 7602 [42].

Physical Principle

Molecular bonds vibrate at various frequencies depending on the elements and the type of bonds. For any given bond, there are several specific frequencies at which it can vibrate. According to quantum mechanics, these frequencies correspond to the ground state (lowest frequency) and

several excited states (higher frequencies). One way to cause the frequency of a molecular vibration to increase is to excite the bond by having it absorb light energy. For any given transition between two states the light energy (determined by the wavelength) must exactly equal the difference in the energy between the two states [usually ground state (E_0) and the first excited state (E_1)] [43]. The energy corresponding to these transitions between molecular vibrational states is generally 1-10 kilocalories/mole which corresponds to the infrared portion of the electromagnetic spectrum.

Sample preparation

Samples for FTIR can be prepared in a number of ways. For liquid samples, the easiest is to place one drop of sample between two plates of sodium chloride (salt). Salt is transparent to infrared light. The drop forms a thin film between the plates. Solid samples can be milled with potassium bromide (KBr) to form a very fine powder. This powder is then compressed into a thin pellet which can be analyzed. KBr is also transparent in the IR.

3.4.3 Mechanical Profilometer (Thickness Measurement)

There are many different optical (classical interferometry, holographic interferometry, moiré methods, speckle techniques and white light interferometry) and mechanical techniques used to measure surface shape and roughness.

Talysurf series 2 instrument mechanical profilometer was used to measure the thickness and surface finish. Here mechanical transducer, called a stylus, is dragged across a surface and its movement in the vertical direction is recorded to obtain a surface profile. Stylus (90° conical diamond stylus with the spherical tip of 2 mm radius) is carried at one end of a beam pivoted at the fulcrum on knife edges. The remote end carries an armature which moves between two coils, changing their relative inductance.

.

Photograph 3.3 Mechanical Profilometer

The signal is amplified by special gauges are also used in the newer types of measuring instruments, where the range to resolution ratio has increased from approx 1000:1 to better than 64 000:1. It means that 0.6 nm resolution can be reached for range 0.03 mm (z). A maximal nominal measuring range (z) is 0.8 mm. The traverse length interval is 120 mm/0.1 mm (Xmax/Xmin), data sampling interval is 0.25 mm for traverse length to 30 mm and 1 mm for length over 30 mm. Surface texture parameters are obtained from the digitalized signal, for peak parameters with uncertainty 2%+4nm. Instrument is controlled by Ultra software, it incorporates calibration and measurement functions too [44].

3.4.4 Thermogravimetry Analysis (TGA)

The Q600 Simultaneous TGA/DSC (SDT) provides simultaneous measurement of weight change (TGA) and differential heat flow (DSC) from ambient to 1500 °C. SDT technology features a dual beam thermobalance that compensates for beam growth and buoyancy contributions to baseline drift; thermocouples that provide differential temperature measurements (DTA) within the dual ceramic beams; and a purge gas system with digital mass flow control, gas switching capability and a separate gas inlet for the option to deliver reactive gas to the sample. For analyzing samples that tend to lose weight during heating, the new Q600 technology provides improved DSC accuracy when the instantaneous weight, rather than the initial sample weight, is

used in heat flow integration. The DSC signal is also useful in providing higher temperature solid state phase and melting transitions where no weight loss occurs.

Thermogravimetry analysis (TGA) is a technique by which the mass of a material is measured as a function of temperature while the material is subjected to a controlled temperature program. On the TGA curves the mass is normally plotted on the Y-axis and temperature is on X-axis increasing from left to right

Differential scanning calorimeter (DSC) measure the difference in energy input into a substance and a reference material as a function of temperature while the substance and reference are subjected to a controlled temperature program

Photograph 3.4 Thermal Analysis Instrument

There are two modes of DSC one is Power Compensation DSC another is Heat Flux DSC. On removing the thermocouple from direct contact with the samples and introducing controlled heat leak between the sample and the reference container is refer to as Heat-Flux DSC. In case of power compensation DSC has been used to separate heaters for sample and reference container with the differential power needed to keep the sample and reference at same temperature.

3.4.5 Transmission Electron Microscope (TEM)

Transmission Electron Microscope was used to analyze the thin composite films. Here Hitachi model no H7600 was used to analyze the composite.

Transmission electron microscopy (**TEM**) is a microscopy technique whereby a beam of electrons is transmitted through an ultra thin specimen, interacting with the specimen as it passes through. An image is formed from the interaction of the electrons transmitted through the specimen; the image is magnified and focused onto an imaging device, to be detected by a sensor such as a CCD camera

TEMs are capable of imaging at a significantly higher resolution than light microscopes, owing to the small de Broglie wavelength of electrons. This enables the instrument to be able to examine fine detail even as small as a single column of atoms, which is tens of thousands times smaller than the smallest resolvable object in a light microscope. TEM forms a major analysis method in a range of scientific fields, in both physical and biological sciences. TEMs find application in cancer research, virology, materials science as well as pollution and semiconductor research

The advantages of **Transmission electron microscope** over optical microscope is due to two major factors which are:

1) The electron beam is influenced by electric and magnetic field, so the magnetic lenses that we use in TEM are free from all the spherical and chromatic aberration.

2) Theoretically, the maximum resolution that one can obtain with a light microscope has been limited by the wavelength of the photons that are being used to probe the sample, which is of 400–700 nm. But with the help of an electron beam we can reach 4 to 10nm by applying a very high electric potential (100KV)

So, the resolution of optical Microscope is limited by diffraction of light. No microscope has yet been built for “light” of even shorter wavelengths (i.e. X-rays)- it is difficult to make lenses for X-rays One of the basic discovery of Quantum Physics is that particle with a mass m and velocity v can behaves as wave with wavelength

Electron which are accelerated by a potential difference of 100kV have λ = 0.004nm (approx.) i.e. 1/15 of atomic diameter. Science magnetic lenses are always positive it is not possible to compensate for lens aberration in same way as in optical microscope. Aberration & wavelength therefore limit the theoretical resolution of electron microscope of approx 0.2nm (i.e. atomic diameter).

3.4.6 Dielectric Measurement

The study of dielectric behavior of PANI and PANI–ZnO composites were carried out by HIOKI3532-50 LCR HiTESTER.

Photograph 3.5 LCR setup.

Network Analyzer consists of signal source, receiver and a display. Signal source produces a signal at a particular frequency which is coupled to the material under test and the receiver is tuned to that frequency to detect the reflected and transmitted signals from the material and provides the magnitude and phase data at that frequency

A capacitor consists of two conductors separated by a non-conductive region. The non-conductive substance is called the dielectric medium, although this may also mean a vacuum or a semiconductor depletion region chemically identical to the conductors. A capacitor is assumed to be self-contained and isolated, with no net electric charge and no influence from an external

electric field. The conductors thus contain equal and opposite charges on their facing surfaces, and the dielectric contains an electric field. The capacitor is a reasonably general model for electric fields within electric circuits.

An ideal capacitor is wholly characterized by a constant capacitance C, defined as the ratio of charge $\pm Q$ on each conductor to the voltage V between them:

$$C = \frac{Q}{V}$$

Sometimes charge buildup affects the mechanics of the capacitor, causing the capacitance to vary. In this case, capacitance is defined in terms of incremental changes

When a dielectric is subjected to an a.c. field the displacement of charges and ions and orientations of dipole moments must vary in direction periodically. The switching of the displacements and the orientation with the fast reversal of the electric field becomes more difficult at higher frequencies. Dielectrics are subjected to high frequency electric fields, when high frequency electromagnetic radiation is incident on them. The charges and electric dipoles in the dielectric respond to the oscillating electric field of electromagnetic radiation. From electromagnetic theory, it can be shown that the dielectric constant in the optical frequency range is closely related to refractive index of the material and is equal to the square of it.

Among the three types of polarizabilities, the electronic polarizability which involves electrons is a fast process and so the electronic polarizability exists up to very high frequency at a.c. fields, even up to U.V range. The ionic and dipolar polarizabilities which involve ions and dipoles are slower process due to the inertia of the ions and molecular dipoles. The dipolar polarizability which is due to the orientation due to the dipoles is the slowest process. The dipoles can not respond beyond the microwave frequency. Above microwave frequency, the contribution of the total polarizability is only from ionic and electronic process. The ionic contribution exists up to infrared frequencies. Beyond infrared, the displacement of ions can not respond fast enough due to inertia of ions. So, the contribution beyond infrared is only due to electronic polarizability.

3.5 SYNTHESIS OF COMPOSITE

3.5.1 Synthesis of PANI

Synthesis of Polyaniline involves various steps:

- Preparation of 1 molar HCl solution,
- 0.2 molar aniline solution and
- 0.2 molar ammonium persulfate solution.

Polyaniline has been synthesized by chemical oxidative polymerization method. For the synthesis of polyaniline 0.1M aniline 2.0M HCL in double distilled water was taken. These were stirred in a beaker which was kept inside the rubber insulator at 0^0C. After this, 8gm ammonium peroxidisulphate was dissolved in minimum (30-40 ml/gm) quantity of water. The ammonium peroxidisulphate is then added drop wise to above insulated beaker with constant stirring. The color changes to dark green. This solution was put for over night. The solution was then filtered in Butchner funnel and the residue was washed 2-3 times with distilled water in the same funnel. The filtered residue is the dried for 4-5h in electrical oven at 50^0 C.

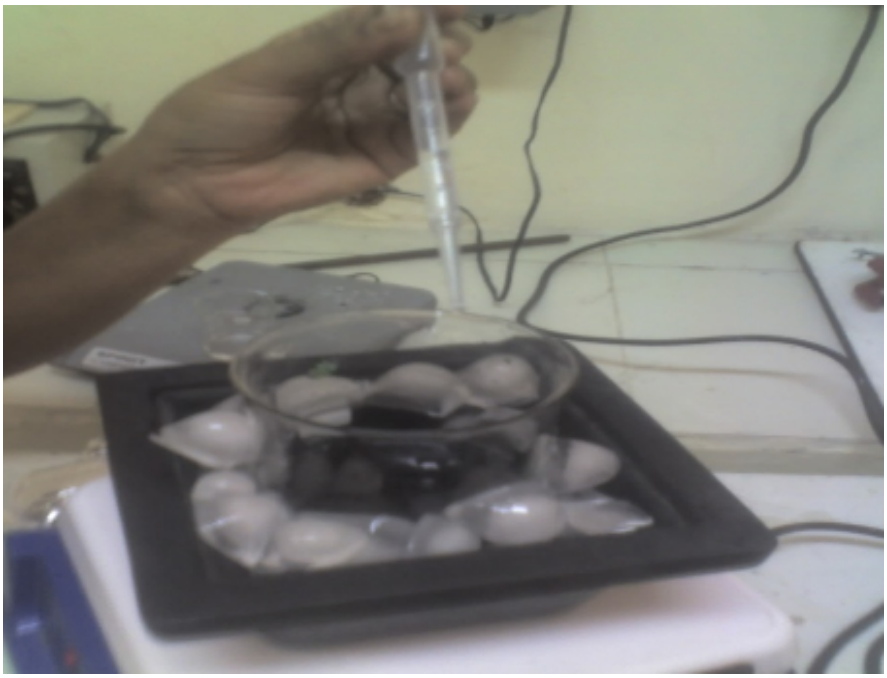

Photograph 3.6 Synthesis of PANI.

3.5.2 Synthesis of ZnO Nanoparticles

ZnO nanoparticle synthesis was as follow Zinc acetate dihydrate (3.35 mmol) was first dissolved in methanol (31.25 ml) and another solution of potassium hydroxide was prepared by dissolving potassium hydroxide (6.59 mmol) in methanol (16.25 ml). The potassium hydroxide solution was added dropwise to the zinc acetate solution at 60◦C under vigorous stirring. After 1.5 h, nanoparticles started to precipitate and the solution became turbid. The heater and stirrer were removed after 2 h and the solution was allowed to sit for another 2 h. The ZnO nanoparticles settled at the bottom and the excess mother liquor was removed and the precipitate was washed twice with methanol (12.5 ml). The precipitate was then dispersed in 12.5 ml of methanol and 2.5 ml of chloroform. The dispersed solution was translucent and stable for up to 2 weeks [45].

3.5.3 Synthesis of PANI-ZnO composite

The undoped polyaniline powder was dissolved in N-methyl-2-pyrolidone. The solution was stirred for 6 hrs and filtered by a whatman filter paper having pore size of 6micron. A film of this undoped PANI was deposited by spin coating method on a glass substrate with 600 rpm for 20 sec and then dried at 1500 rpm for 45sec. The film was then put for half an hour to dry completely at room temperature. A free standing film was also deposited by solution casting technique. For this a glass slides were taken in a Petri dish and spread the solution over them by a dropper.

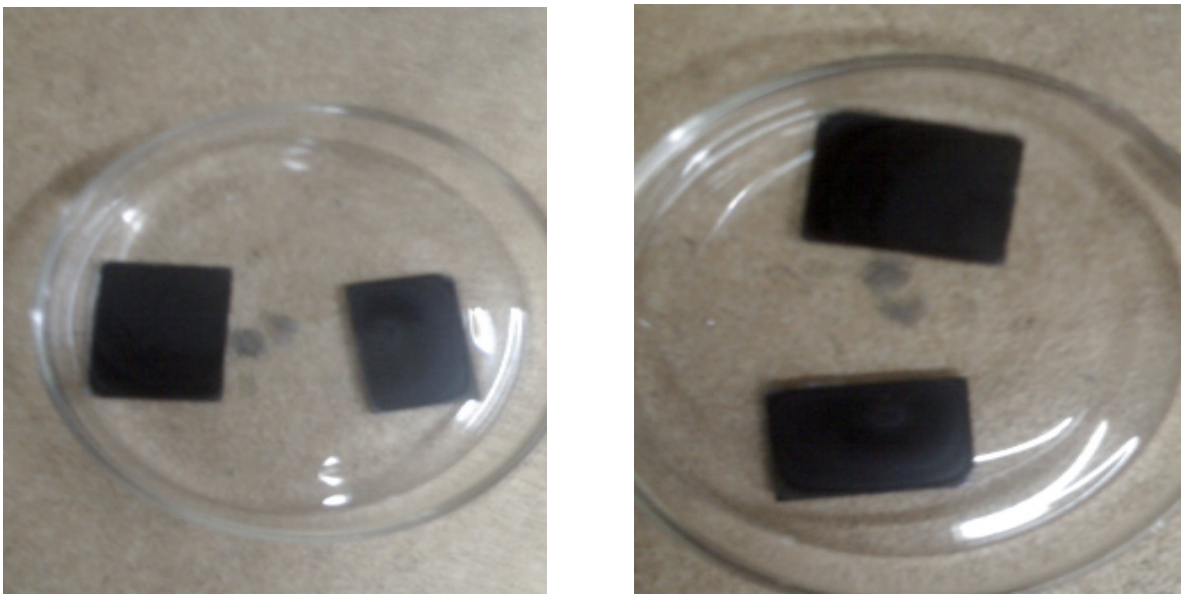

Photograph 3.7 Thin film of PANI-ZnO composite.

The ZnO composites with undoped PANI were prepared by adding 20% ZnO and 30 % ZnO in filtered solution of undoped PANI in NMP. After that the solution was arranged on the magnetic stirrer for 5 hrs. The film of composites were prepared on glass substrate by spin coating method at 600 rpm for 20sec and then dried at 1500 rpm for 45sec. Other free standing films of composite were also prepared by the solution casting technique [37].

CHAPTER-4

RESULTS AND DISCUSSION

CHAPTER-4

RESULTS AND DISCUSSION

4.1 INTRODUCTION

This chapter carries the detail discussion of the results which are shown by various characterization techniques. The new composite which has been developed will be verified by the results if the various characterization techniques. The different results of the composite material will be compared with its matrix material and particulate materials.

4.2 XRD ANALYSIS

XRD analysis of bulk film of composite was conducted over the glass substrate. The characteristics peaks of ZnO comes at 31.72^0, 34.5^0, 36.3^0, 47.76^0, 56.6^0, 63.1^0 and 68^0 which corresponds to miller indices (100) (002) (101) (102) (110) (103) and (201), respectively. The average crystallite size was calculated by using Scherer formula by measuring the full width at half maxima of the (101) peak. The average size was found to be 27nm. This is further confirmed by TEM results.

The XRD pattern of PANI shows a broad peak at $2\theta=19^0$, which corresponds to (200) plane of PANI. The XRD pattern of ZnO powder and PANI-ZnO (20%) composite exhibit the characteristic peak for crystalline ZnO of wurtzite structure this indicates that crystal structure of ZnO is not modified due to the presence of PANI. All the peaks of PANI-ZnO composites shift slight higher values of 2θ. From the XRD peaks it was observed that lattice parameter for ZnO were $a=b=3.2269A^o$ and for composite were $a=b=3.2442A^o$, $c=5.2061A^o$. This change of lattice parameter shows that the unit cell of ZnO stretches along horizontal plane and suppresses along c-axis. Since the surface area along the horizontal direction of unit cell is more than that of combined surface area of two vertical surfaces (top and bottom). So, more of the PANI chains are expected to attach on horizontal surface. Due to that attachment of PANI chains ZnO unit cell suppressed along c-axis and stretches along horizontal direction.

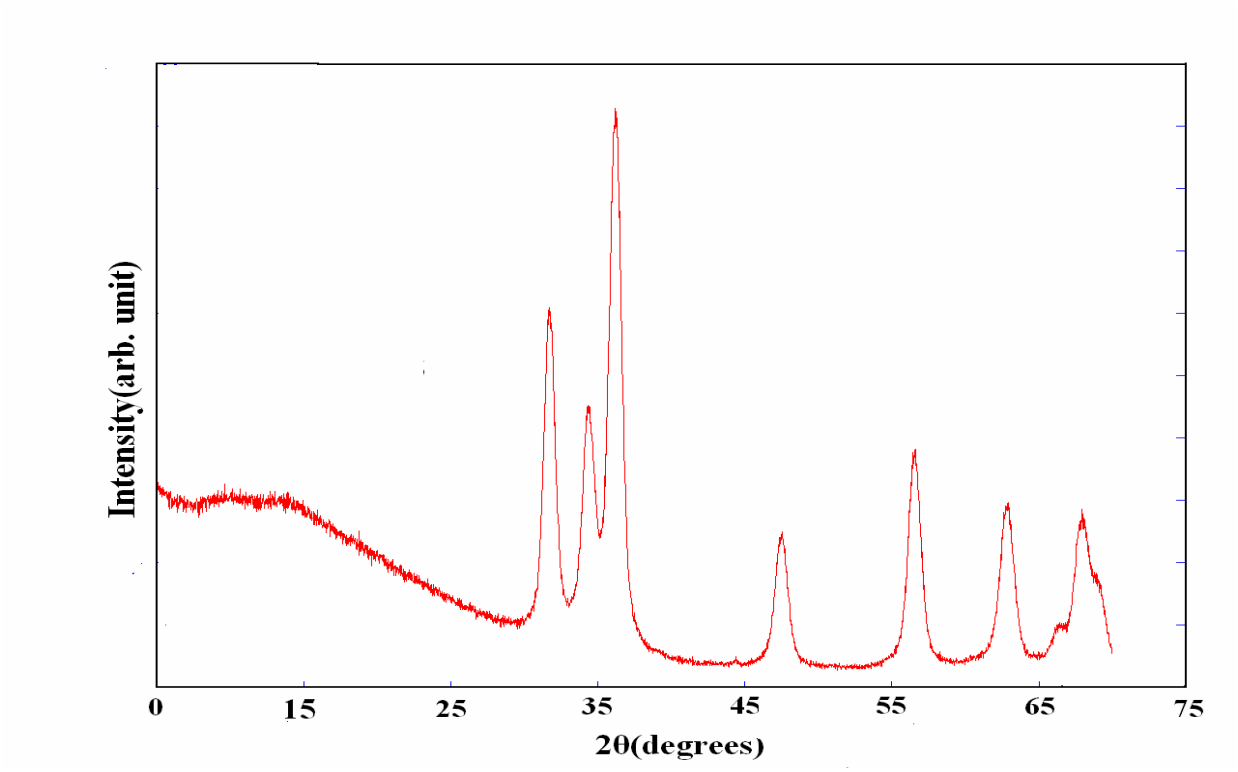

Fig.4.1 XRD pattern of ZnO nanoparticles.

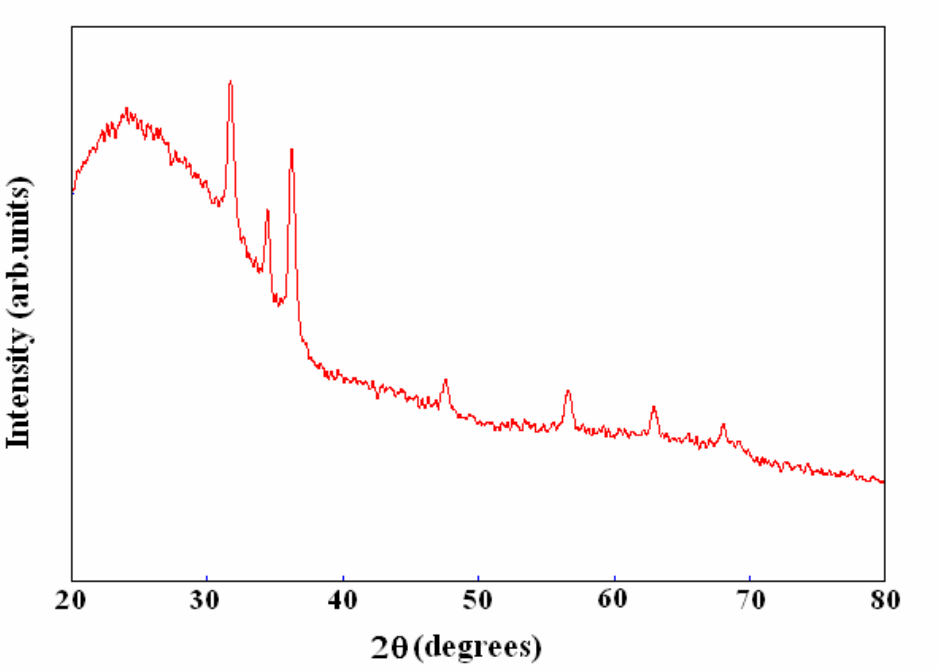

Fig.4.2 XRD pattern of PANI-ZnO composite.

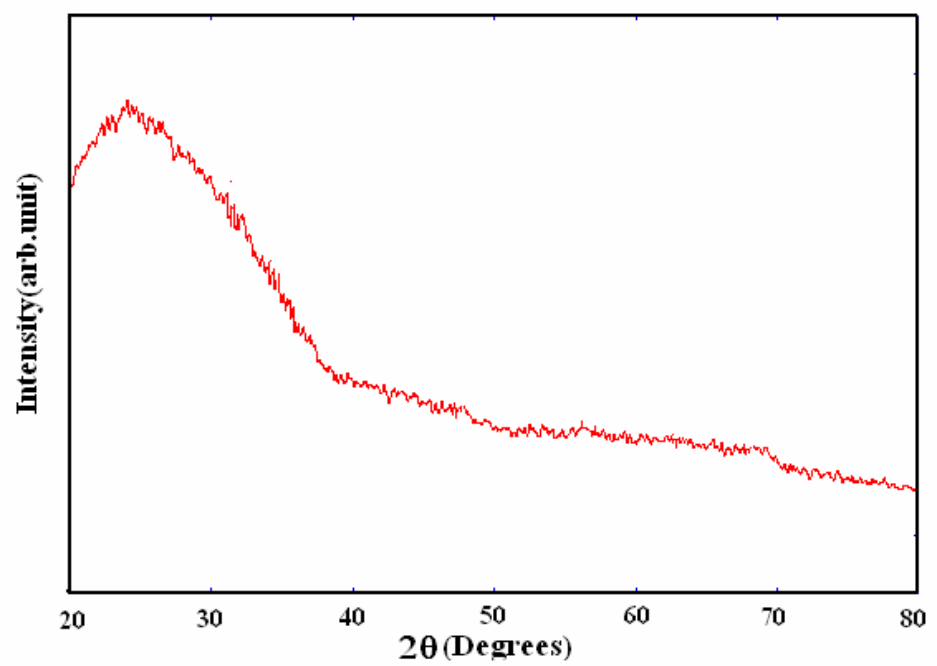

Fig.4.3 XRD pattern of PAN

4.3THICKNESS MEASUREMENT

Thickness of PANI-ZnO composite film was measured with the help of mechanical profilometer. The graph given below can be used to measure thickness. Here on going from left to right we have a step at the origin. This step is the measure of thickness of film and can be measured by subtracting lower-right value from upper-left value. So, the thickness is

$$\Delta t = 34.0869 -- 29.0907\mu m$$

$$t = 4.9962\mu m$$

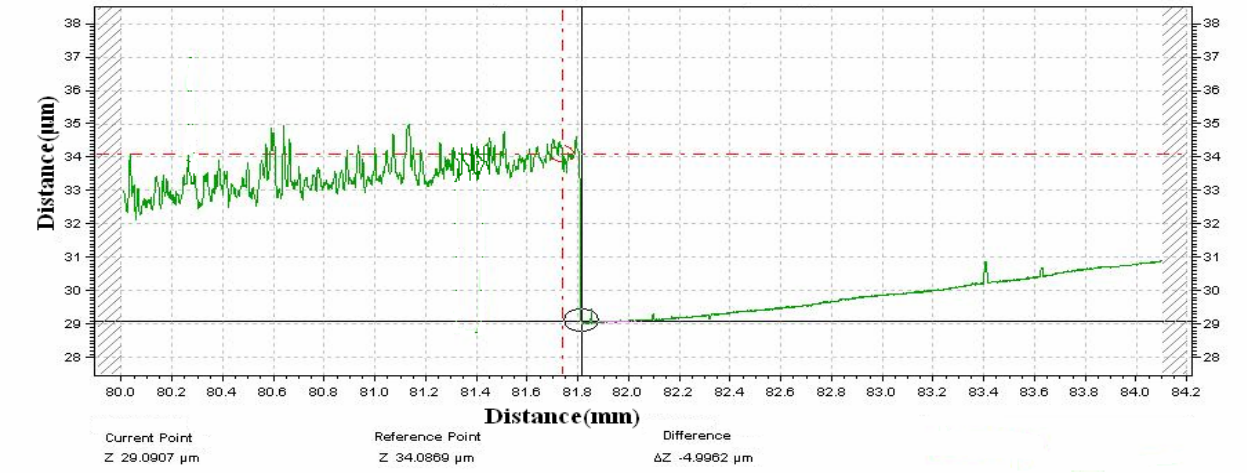

Fig.4.4 Measurement for thickness of thin film.

Also the measurement of roughness was as shown in fig. 4.4.

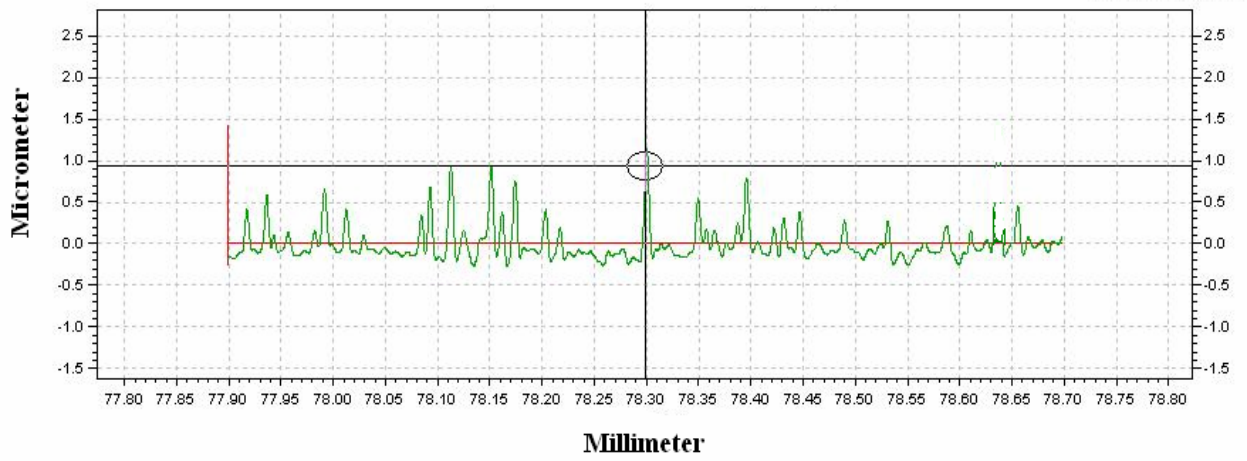

Fig.4.5 Measurement of surface roughness.

4.4 TGA

The TGA plot of ZnO-PANI composite was carried out in the presence of Nitrogen from 30^{o}C to 1000^{o}C. For PANI initially the huge loss of weight (97.32%) up to the temperature of 160^{o}C is due to the loss of NMP from melt. After that there was no change in weight up to the temperature 430^{o}C, which shows that the PANI is stable up to that temperature. After this PANI starts to decompose at 480^{o}C. The reaction completes at 600^{o}C.

For PANI-ZnO composite the curve was nearly same and loss of weight occurs due to loss of NMP (97.13%) upto 175^{o}C temperature. After that there was no weight change till 445^{o}C temperature was reached (430^{o}C for PANI). This shows that composite was stable till that temperature and strength of composite also increased due to the attachment of PANI chains with ZnO crystallites. The composite decompose 0.88% up to the temperature of 637^{o}C (which was 600^{o}C for PANI). After 637^{o}C temperature there was no weight change up to 1000^{o}C that was because of the stability of ZnO nanoparticles.

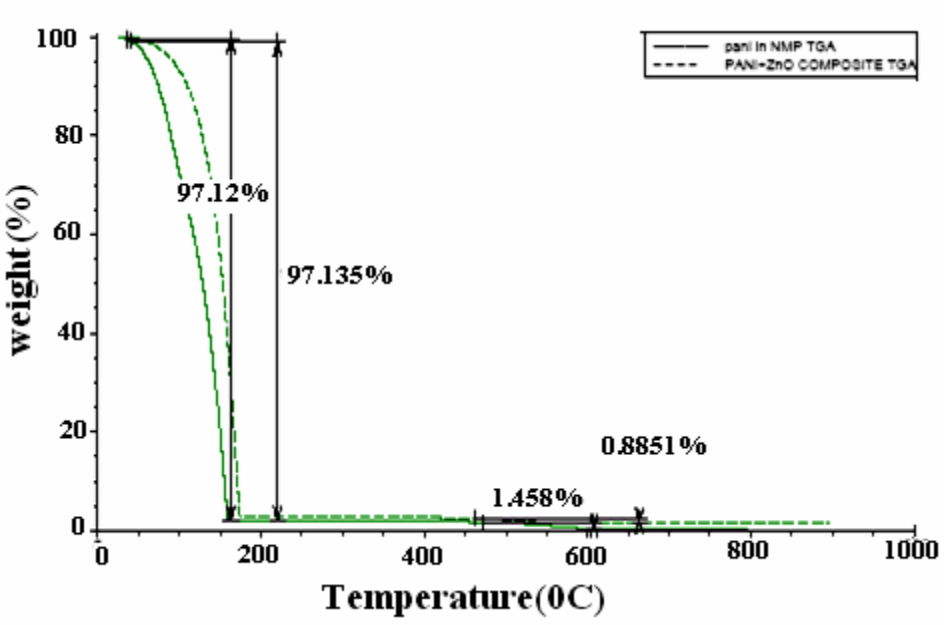

Fig. 4.6 TGA

4.5 FTIR SPECTRAL STUDIES

FTIR spectra of pure PANI and PANI-ZnO(20%) composite in KBr is given in the fig. 4.7 and 4.8 the characteristics peaks of PANI at 503.1cm^{-1}, 587.6 cm^{-1},798.7 cm^{-1}, 1121.8 cm^{-1}, 1296.7 cm^{-1}, 1472.4 cm^{-1}, 1559.8 cm^{-1}, 2369.3 cm^{-1} and 3446.7 cm^{-1} corresponds to the C = N iminoquinone, C =C stretching mode of quinoid rings, the C = C stretching mode of the benzenoid rings, the stretching mode of C – N, the stretching mode of N = Q = N where Q represents the quinoid ring and C – H bonding mode of aromatic rings The PANI-ZnO composite also shows the same characteristics peaks. But the corresponding peaks of pure PANI at 798.7 cm^{-1}shifted to 794 cm^{-1},1121.8 cm^{-1} shifted to 1136 cm^{-1}, 1472.4 cm^{-1} shifted to 1490.2 cm^{-1}and 1559.8 cm^{-1} shifted to1580.2 cm^{-1} wave numbers in PANI-ZnO composite. The shift may be described due to the formation of hydrogen bonding between ZnO and NH group of PANI on the surface of ZnO particles. Such kind of interaction is observed by other researchers also [46].

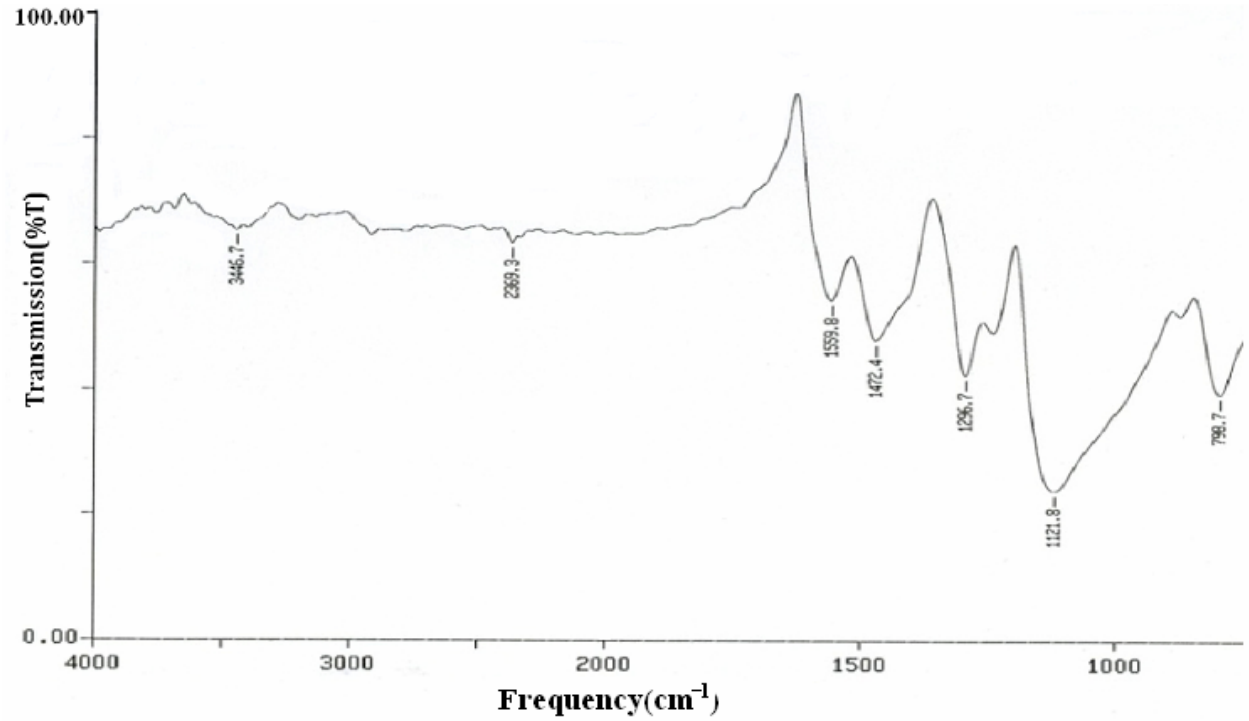

Fig. 4.7 FTIR Spectra of PANI.

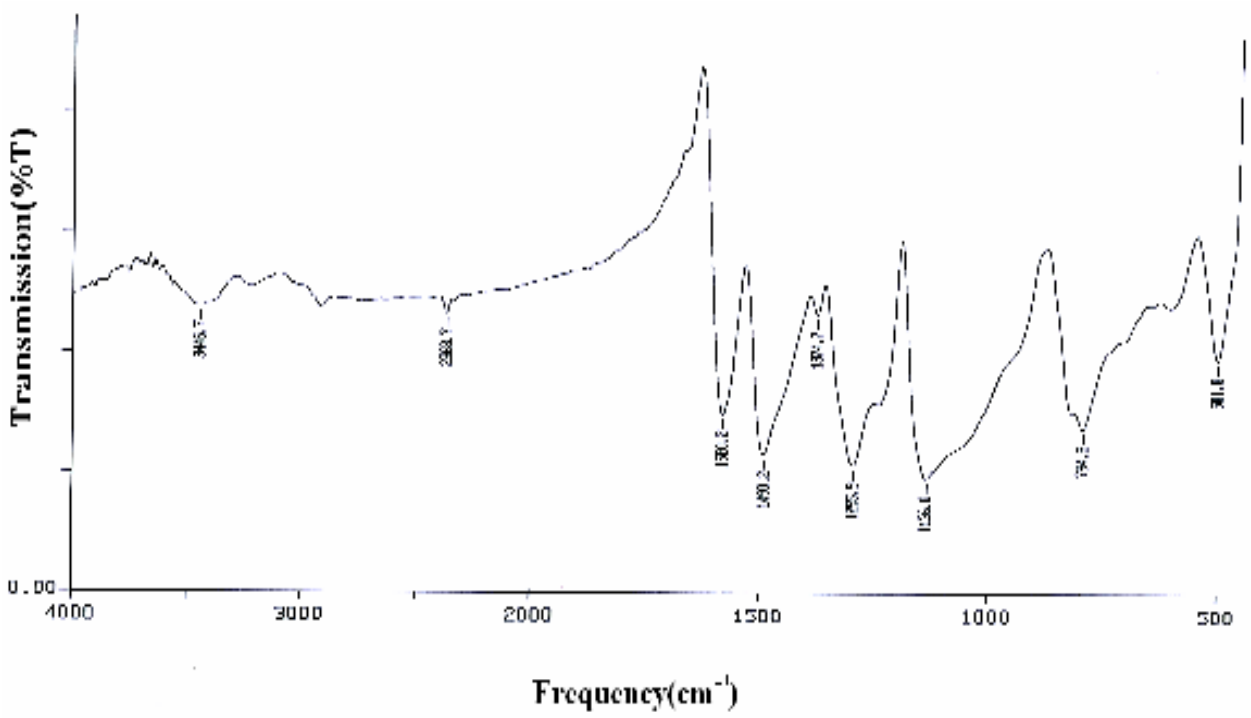

Fig. 4.8 FTIR Spectra of PANI-ZnO composite.

4.6 Dielectric behavior

The behavior of dielectric constant (ε) of PANI and PANI–ZnO composites as a function of frequencies (1 to 800 kHz) are shown in Fig. 4.9.

For PANI the dielectric constant as a function of frequency decreases from 674.34 to 604.17 while for PANI–ZnO (20%) composite and PANI–ZnO (30%) composite, it remains almost constant. The real part of permittivity of PANI–ZnO (20%) composites decreases by a factor of □2 and for PANI–ZnO (30%) composite by □9 in comparison of pure PANI. This decrease in real part of permittivity can be explained by the multi-core model of interface between ZnO particle and PANI. According to this model the interface between particles and polymer consists of multilayer in which the inner layer consists of polymer chains. These layers are strongly attached to the surface of ZnO particles and the outer layer consists of polymer chains which are loosely interacted to the inner layer. It is characterized by different chain conformation, chain mobility and free volume. The reduction in the real part of permittivity is related to inner bound layer which impairs the motion of dipoles and the free volume contributed by the outer layer. In the present case of PANI–ZnO composite, there is a strong interaction on the surface of ZnO particles with the PANI molecular chains as indicated by the XRD and FTIR analysis. The reason of this interaction may be attributed to the defects on the surface of ZnO particles. These defects may act as active sites (dipoles) for the interaction of PANI molecular chains. The adsorption of PANI molecular chains at the defects sites provides the prevention of motion of dipoles giving less contribution to the net polarization and thus leads to the reduction in ε. In the outer layer, the attachment of PANI molecular chains to the inner layer or to the surface of the ZnO particle is weak. Due to the weak interaction, PANI molecular chains are scattered, providing more voids between the PANI molecular chains, giving a reasonable contribution to the free volume and hence the reduction in ε [37].

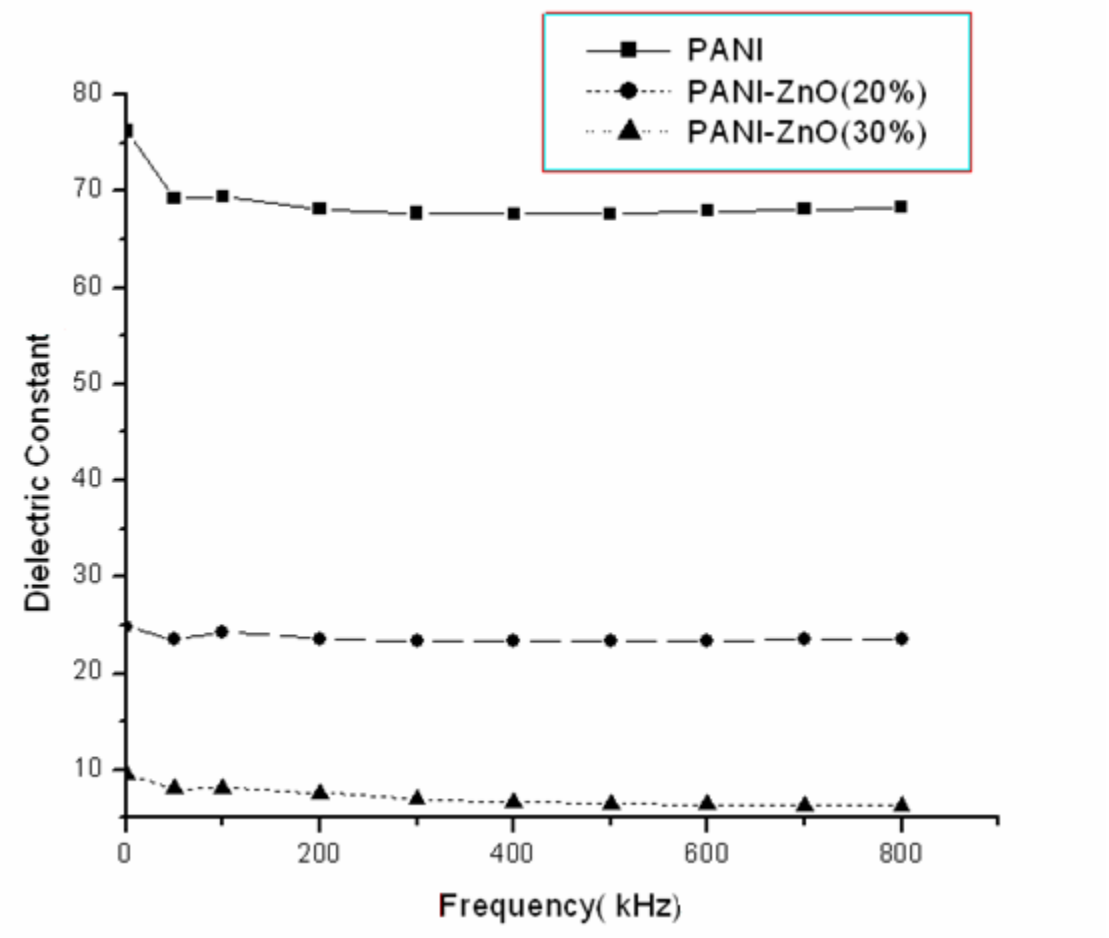

Fig. 4.9 Variation of dielectric constant with frequency.

4.7 TEM Analysis

The fig 4.10 shows the TEM images of ZnO nanoparticles. It is clear from the image that shape of particles is spherical, the average size of particles lies between 5 to 10 nm in diameter. The dark images show that nanoparticles are solid in structure. The TEM images (Fig. 11 (a), 11 (b)) of PANI-ZnO composite shows that particles are entrapped inside the matrix of PANI and size of particles is same so there is no agglomeration of ZnO nanoparticles in PANI matrix. Also, the distribution of ZnO particle in PANI matrix is nearly uniform.

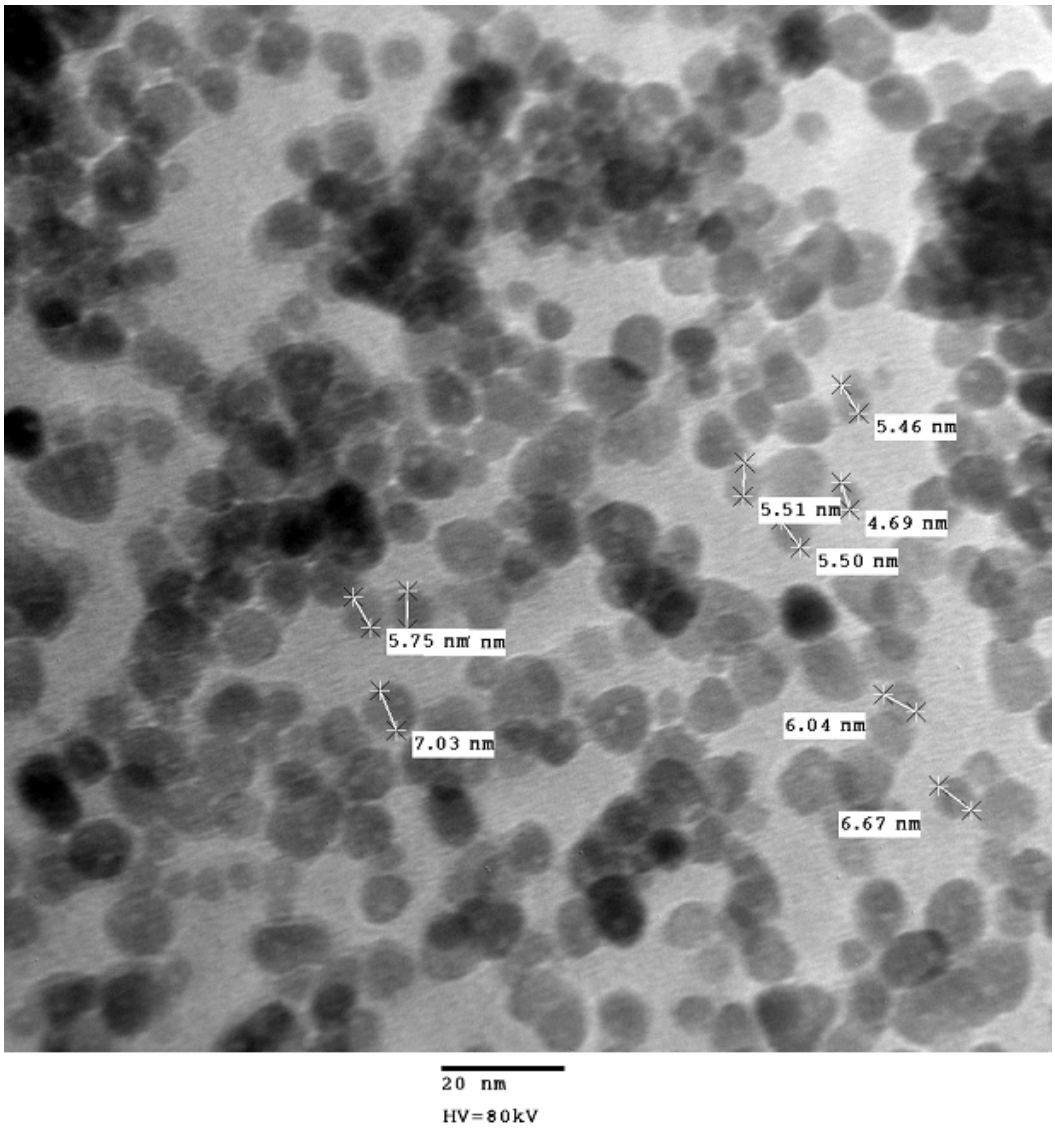

Fig.4.10 TEM image of ZnO nanoparticles.

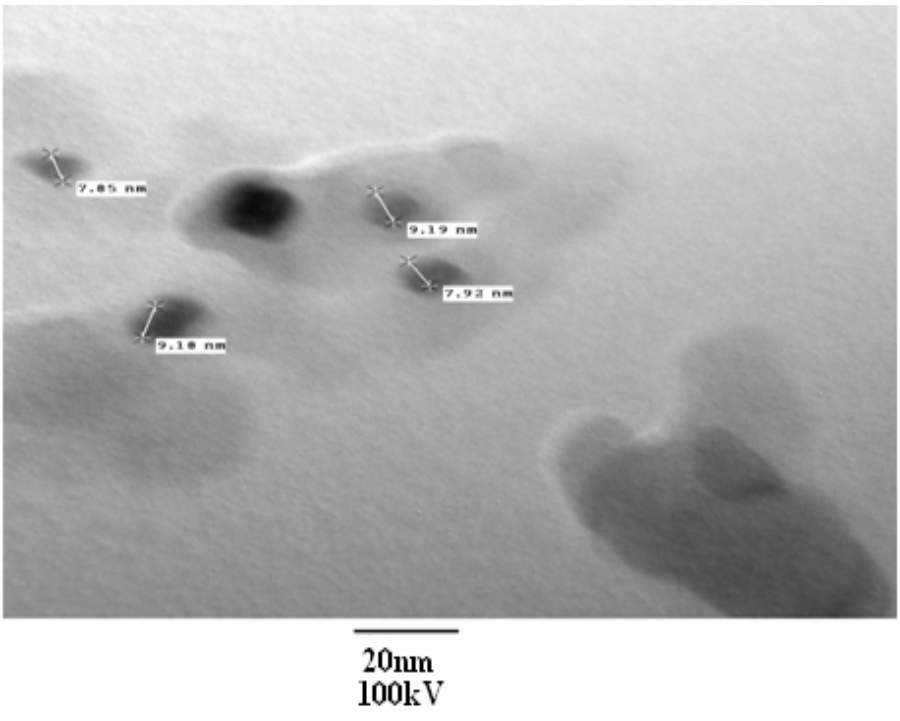

Fig. 4.11(a) TEM image of PANI-ZnO composite.

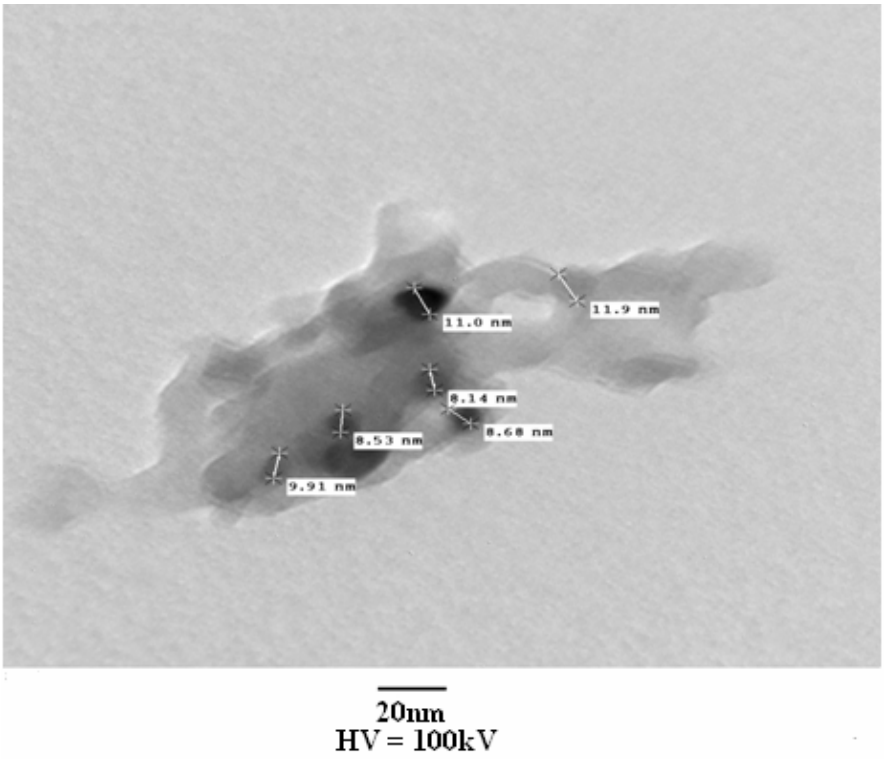

Fig. 4.11(b) TEM image of PANI-ZnO composite.

CHAPTER-5

CONCLUSIONS

AND

FUTURE SCOPE

CHAPTER-5

CONCLUSIONS AND FUTURE SCOPE

CONCLUSIONS

Films of polyaniline and polyaniline–ZnO composites were synthesized by solution casting techniques. Films are deposited over glass and ITO/glass substrate. The measured thickness of composite films was in micrometer range. The TEM images show that ZnO nanoparticles are spherical in shape and dark images shows that they were solid. The TEM study of PANI–ZnO composite film revealed uniform distribution of ZnO particles in PANI matrix. The absorption peaks in FTIR spectra of PANI–ZnO composite film were found to shift to higher wavenumber as compared to those observed in pure PANI. The observed shifts were attributed to the interaction between the ZnO particle and PANI molecular chains. A change in the value of lattice parameter of ZnO in the PANI–ZnO composite was observed which also indicated the presence of interaction between ZnO particles and PANI matrices. The dielectric study of PANI and PANI–ZnO composites revealed decrease of dielectric constant of PANI after the formation of PANI–ZnO composite which is attributed to the interfaces formed between ZnO nanoparticles and PANI.

FUTURE SCOPE

The dielectric properties and losses of a material are much relevant for telecommunication applications in aerospace and for EMI shielding. A low dielectric constant is often desirable for several applications for example, high-speed integrated packages require materials with dielectric constant lower than 3.5, whereas satellite communication applications require materials with a dielectric constant of 2.5 in addition of low loss.

The range of organic molecules displaying substantial semiconducting action in TFTs has been expanded to include various shapes and constitutions. Several approaches to high hole mobility have been uncovered, and electron mobility may also now be seriously considered.

The polyaniline is a p-type semiconductor and the ZnO is an n-type semiconductor. Current-voltage measurements are done at 25◦C or about 298K. The samples have rectifying behavior and are similar to the I-V plots of the rectifier diodes commonly used in electronic circuits.

The non-linear electrical characteristics of a polymeric electrochemically controlled junction based on a conducting polymer (polyaniline) and a solid electrolyte (Li+ doped polyethylene oxide) are considered as basic features for the realization of smart materials.

In recent years, the development of inorganic/polymer hybrid materials on nanometer scale have been receiving significant attention due to a wide range of potential applications in optoelectronic devices and in field effect transistors.

.

REFERENCES

[1] Self doped conducting polymers by Michael S.Fruend and Bhavana Deore (2007) 20-25.

[2] H. Shirakawa, E. J. Louis, A. G. MacDiarmid, C. K. Chiang, A. J. Heeger, Chemical Communications (1977) 578.

[3] A. J. Heeger, Angewandte Chemie – International Edition 40 (2001) 2591.

[4] H. Letheby, Journal of the Chemical Society 15 (1862) 161.

[5] A. O. Patil, A. J. Heeger, F. Wudl, Chemical Reviews 88 (1988) 183.

[6] C. K. Chiang, C. R. J. Fincher, Jr., Y. W. Park, A. J. Heeger, H. Shirakawa, E. J. Louis, S. C. Gau, A. G. MacDiarmid, Physical Review Letters 39 (1977) 1098.

[7] H. Shirakawa, Angewandte Chemie – International Edition 40 (2001) 2575.

[8] Y. Cao, J. J. Qiu, P. Smith, Synthetic Metals 69 (1995) 187.

[9] J. L. Bredas, G. B. Street' Accounts of Chemical Research 18 (1985) 309.

[10] A. Pron, P. Rannou Progress in Polymer Science (2002) 27 135.

[11] W. P. Su, J. R. Schrieffer, A. J. Heeger, Physical Review Letters 42 (1979) 1698.

[12] C. Rebbi, 'Solitons,' Scientific American 240 (1979) 92.

[13] A. F. Diaz, K. K. Kanazawa, G. P. Gardini, Chemical Communications 14 (1979) 635.

[14] A. G. MacDiarmid, Angewandte Chemie – International Edition 40 (2001) 2581.

[15] E. Menefee, Y. H. Pao, Journal of Chemical Physics 36 (1962) 3472.

[16] V. V. J. Walatka, M. M. Labes, J. H. Perlstein, Physical Review Letters 31,

[17] W. D. Gill, W. Bludau, R. H. Geiss, P. M. Grant, R. L. Greene, J. J. Mayerle, G. B. Street,Physical Review Letters 38 (1977) 1305.

[18] G. Natta, G. Mazzanti, P. Corradini, 'Stereospecific polymerization of acetylene,' Atti accad. nazl. Lincei Rend. 25 (1958) 3.

[19] C. K. Chiang, S. C. Gau, C. R. J. Fincher, Y. W. Park, A. G.MacDiarmid, A. J. Heeger, Applied Physics Letters 33 (1978) 18.

[20] R. B. Seymour, Conductive Polymers; Polymer Science and Technology, 1st edn, Plenum Press, New York, 1981.

[21] R. Dupon, D. H. Whitmore, D. F. Shriver, Journal of the Electrochemical Society128 (1981) 715.

[22] J. STEJSKAL Pure and Applied Chemistry 74 (2002) 857-867.

[23] N. Gospodinova, and L.Terlemezyan, Prog. Polym. Sci. 21 (1998) 443.

[24] A.Dall'olio, Y.Dascola, V.Varacca and V.Bocchi, Comptes Rendus 267 (1968) 433.

[25] R. K. Yuan, S. C. Yang, H. Yuan, R. L. Jiang, H. Z. Qian, D. C. Gui, Synthetic Metals 41 (1991) 727.

[26] Y. Jiang, A. J. Epstein, Journal of the American Chemical Society 112 (1990) 2800.

[27] J. Y. Bergeron, J. W. Chevalier, L. H. Dao, Chemical Communications (1990) 180.

[28] C.J. Mathal, S. Saravanan, M.R. Anantharaman, S.Venkitachalam and S. Jayalekshmi, Institute of Physics Publishing, 35 (2002) 240-245.

[29] W. Jakub, J. Stejskal, O. Quadrat, P. Kratochvil, and P. Saha, Croatica Chemica ACTA, 71 (1998) 873-882.

[30] S. Bekir and M.Talu, Turk J Chem, 22 (1998) 301-307.

[31] Hadi Nur, Norizah Abdul Rahman, Salasiah Endud, Lim Kheng Wei. Applied Chemistry 29 (1999) 759-764.

[32] R. Del RIÂO1, J.H. ZAGAL1, G.de T. ANDRADE2 and S.R. BIAGGIO2 Journal of Applied Chemistry 29 (1999) 759-764.

[33] Y.-N. Qi, F. Xu1, H.-J. Ma, L.-X. Sun1, J. Zhang1,3 and T. Jiang1,3 Journal of Thermal Analysis and Calometry,91 (2008) 219-223.

[34] Neelgund, Gururaj M; Hrehorova, Erika; Joyce, Margaret; Bliznyuk, Valery Polymer International 57 (2008) 1083-1089.

[35] Shiv P. Sharma, M.V.S. Suryanarayana , Anil K. Nigam, A.S. Chauhan, L.N.S. Tomar Catalysis Communications 10 (2009) 905–912.

[36] Jui Hung Chen a, Chu-Yun Cheng a, Wen-Yen Chiu a,b, Chia-Fen Lee c, Nai-Yun Liang European Polymer Journal 44 (2008) 3271–3279.

[37] Bhupendra K. Sharmaa, Ajai K. Gupta b, Neeraj Kharea, S.K. Dhawanb, H.C. Gupta Synthetic Metals159 (2009) 391-395.

[38] Introduction electrodynamics, David J. Griffiths. Pearson education (2004) 36.

[39] H. P. Klug, L.E. Alexander, \X-ray Di®raction Procedures for Polycrystalline and Amorphous Materials", Wiley, New York, 1954.

[40] L.E.Alexwnder "X-ray diffraction in polymer science" Wiley,LONDON 1969.

[41] F.J.Balta-calleja, C.G.Vonk “X-ray scattering of synthetic polymer.” Elesvier, Amsterdam1989.

[42] P. C. Painter, M. M. Coleman, J. L. Koenig, The Theory of Vibrational Spec troscopy and its Application to the Polymeric Materials", John Wiley & Sons, Chichester 1982.

[43] J. L. Koenig, “Spectroscopy of Polymers", Elsevier, Amsterdam, 1999.

[44] Exploring Surface Texture, a fundamental guide to the measurement of surface finish, published by Taylor Hobson Limited, England, 2003.

[45] Z L S Seow, A SWWong, V Thavasi, R Jose, S Ramakrishna and G W Ho Nanotechnology 20 (2009) 6.

[46] Y.He, applied surface science 249 (2005).